Biogeosciences Discuss., 12, 15411–15460, 2015
www.biogeosciences-discuss.net/12/15411/2015/
doi:10.5194/bgd-12-15411-2015

Biogeosciences Discussions
Open Access

First tephrostratigraphic results of the DEEP site record from Lake Ohrid, Macedonia

N. Leicher[1], G. Zanchetta[2], R. Sulpizio[3,4], B. Giaccio[5], B. Wagner[1], S. Nomade[6], A. Francke[1], and P. Del Carlo[7]

[1]Institute of Geology and Mineralogy, University of Cologne, Zuelpicher Str. 49a, 50674 Cologne, Germany
[2]Dipartimento di Scienze della Terra, University of Pisa, via S. Maria 53, 56126 Pisa, Italy
[3]Dipartimento di Scienze della Terra e Geoambientali, University of Bari, via Orabona 4, 70125 Bari, Italy
[4]Istituto per la Dinamica dei Processi Ambientali (IDPA) CNR, via M. Bianco 9, Milan, Italy
[5]Istituto di Geologia Ambientale e Geoingegneria, CNR, Area della Ricerca di Roma1-Montelibretti, Via Salaria Km 29,300, Roma, Italy
[6]Laboratoire des sciences du climat et de l'environnement, UMR 8212, CEA/CNRS/UVSQ, 91190 Gif-Sur-Yvette, France
[7]Istituto Nazionale di Geofisica e Vulcanologia, Sezione di Pisa, via della Faggiola 32, 56126, Pisa, Italy

Received: 14 August 2015 – Accepted: 25 August 2015 – Published: 17 September 2015

Correspondence to: N. Leicher (n.leicher@uni-koeln.de)

Published by Copernicus Publications on behalf of the European Geosciences Union.

Abstract

A tephrostratigraphic record covering the Marine Isotope Stages (MIS) 1–15 was established for the DEEP site record of Lake Ohrid (Macedonia/Albania). Major element analyses (SEM-EDS/WDS) were carried out on juvenile fragments extracted from 12 tephra layers (OH-DP-0115 to OH-DP-2060). The geochemical analyses of the glass shards of all of these layers suggest an origin from the Italian Volcanic Provinces. They include: the Y-3 (OH-DP-0115, 26.68–29.42 cal ka BP), the Campanian Ignimbrite/Y-5 (OH-DP-0169, 39.6 ± 0.1 ka), and the X-6 (OH-DP-0404, 109 ± 2 ka) from the Campanian volcanoes, the P-11 of the Pantelleria Island (OH-DP-0499, 129 ± 6 ka), the Vico B (OH-DP-0617, 162 ± 6 ka) from the Vico volcano, the Pozzolane Rosse (OH-DP-1817, 457 ± 2 ka) and the Tufo di Bagni Albule (OH-DP-2060, 527 ± 2 ka) from the Colli Albani volcanic district, and the Fall A (OH-DP-2010, 496 ± 3 ka) from the Sabatini volcanic field. Furthermore, a comparison of the Ohrid record with tephrostratigraphic records of mid-distal archives related to the Mediterranean area, allowed the recognition of the equivalents of other less known tephra layers, such as the TM24-a/POP2 (OH-DP-0404, 101.8 ka) from the Lago Grande di Monticchio and the Sulmona basin, the CF-V5/PRAD3225 (OH-DP-0624, ca. 162 ka) from the Campo Felice basin/Adriatic Sea, the SC5 (OH-DP-1955, 493.1 ± 10.9 ka) from the Mercure basin, and the A11/12 (OH-DP-2017, 511 ± 6 ka) from the Acerno basin, whose specific volcanic sources are still poorly constrained. Additionally, one cryptotephra (OH-DP-0027) was identified by correlation of the potassium XRF intensities from the DEEP site with those from short cores of previous studies from Lake Ohrid. In these cores, a maximum in potassium is caused by glass shards, which were correlated with the Mercato tephra (8.43–8.63 cal ka BP) from Somma-Vesuvius. With the tephrostratigraphic work, a consistent part of the Middle Pleistocene tephrostratigraphic framework of Italian volcanoes was for the first time extended as far as to the Balkans. The establishment of the tephrostratigraphic framework for the Lake Ohrid record provides important, independent tie-points for the age-depth model of the DEEP site sequence, which is a prerequisite for

BGD
12, 15411–15460, 2015

paleoclimatic and -environmental reconstructions. Furthermore, this age-depth model will help to improve and re-evaluate the chronology of other, both undated and dated tephra layers from other records. Thus, the Lake Ohrid record is candidate to become the Rosetta stone for the central Mediterranean tephrostratigraphy, especially for the hitherto poorly known and explored lower Middle Pleistocene period.

1 Introduction

Volcanic explosive eruptions produce pyroclastic material, called tephra (gr. $\tau\varepsilon\varphi\rho\alpha$ = ash), which is ejected into the atmosphere and distributed by the prevailing wind systems. Tephra settles down from the atmosphere in a relatively short time (days-weeks) as isochronous event marker horizons into all kind of geological archives downwind of the volcano. By determining the unique geochemical and physical fingerprint of such a tephra horizon, tephra (from different archives) can be characterised, identified, and correlated with each other in order to obtain a tephrostratigraphic framework. If tephra horizons can be dated directly (e.g., $^{39}Ar/^{40}Ar$) or indirectly (e.g., ^{14}C dating on overlying or underlying sediments, varve counting) and correlated with tephra horizons in other archives, also the ages can be transferred to the studied archives.

The Italian volcanism was active during the entire Quaternary (Peccerillo, 2005), which provides an ideal setting for tephrochronological studies (tephrostratigraphy and tephrochronometry, cf. Sarna-Wojcicki, 2013) on a wide spectrum of Quaternary science subjects in the Mediterranean region (Giaccio et al., 2014). After Keller et al. (1978) set up the first tephrostratigraphic scheme for the central Mediterranean region, numerous studies on marine and terrestrial archives have spatially and temporally extended and improved this initial stratigraphy for the Holocene and Late Pleistocene (Paterne et al., 1986, 1988; Vezzoli, 1991; Calanchi et al., 1998; Narcisi and Vezzoli, 1999; Calanchi and Dinelli, 2008; Zanchetta et al., 2011; Tamburrino et al., 2012; Insinga et al., 2014; Satow et al., 2015; Tomlinson et al., 2015).

BGD
12, 15411–15460, 2015

Despite this immense progress over the last decades, tephrochronological work in the period > 200 ka, is still challenging due to incomplete knowledge on the eruption history and limited geochemical analysis. Some records from the Italian Peninsula cover specific intervals of the Early to Middle Pleistocene and can be used as proximal (Karner et al., 2001; Rouchon et al., 2008; Marra et al., 2009, 2014; Palladino et al., 2010; Giaccio et al., 2013a) or mid-distal (Karner et al., 1999; Munno and Petrosino, 2007; Roulleau et al., 2009; Russo Ermolli et al., 2010; Giaccio et al., 2013b, 2014; Petrosino et al., 2014a, b, 2015; Sagnotti et al., 2014) archives of deposits from volcanic complexes. Sediment records spanning continuously > 200 ka are extremely rare in the Mediterranean region. To date, there are only two continuous records covering the entire Middle and Early Pleistocene of the Mediterranean region, which are the Calabrian Ridge core KC01B (Lourens, 2004; Insinga et al., 2014) and the peat record from Tenaghi Philippon, Greece (Tzedakis, 1993; St. Seymour et al., 2004; Pross et al., 2007). However, both records are limited in the tephrostratigraphy to the Holocene and Late Pleistocene.

Lake Ohrid is located on the Balkan Peninsula and is one of the oldest lakes of Europe (Wagner et al., 2014). Over 1.2 Ma of continuous sediments were recovered from Lake Ohrid during the ICDP (International Continental Scientific Drilling Program) deep drilling campaign SCOPSCO (Scientific Collaboration on Past Speciation Conditions in Lake Ohrid). Previous tephrochronological studies on sediment cores from Lake Ohrid covered the last 135 ka and revealed the lake's unique potential as distal tephra archive of Italian volcanoes (Sulpizio et al., 2010).

Here we present first tephrostratigraphic and tephrochronological results of the uppermost 247.8 m composite depth (mcd) of the main drill site (DEEP site) in the central part of the lake, which covers continuously the last ca. 640 ka (Francke et al., 2015). The correlation of the discovered tephra layers to known and dated equivalent tephra horizons from proximal and distal archives enables dating of the Lake Ohrid succession. The transfer of these ages to the Lake Ohrid record provide important, independent tie-points for a tuning based age-depth model (Francke et al., 2015), which is

BGD
12, 15411–15460, 2015

a precondition for environmental and climate reconstructions. The correlation of tephra layers between different geographical archives, both terrestrial and marine, is crucial for a synchronisation of paleoclimatical and paleoenvironmental changes on a regional and global scale.

2 Regional setting

Lake Ohrid (40°54′–41°10′ N, 20°38′–20°48′ E) is located on the Balkan Peninsula (cf. Fig. 1a) and shared between Albania and the Former Yugoslav Republic of Macedonia (FYROM). The lake is 30 km long, 15 km wide and covers an area of 358 km^2, situated at an altitude of 693 m above sea level (a.s.l.). The lake basin has a simple tub-like shape with a volume of 55.4 km^3 and a maximum water depth of 293 m (Lindhorst et al., 2015). Today's water chemistry is oligotrophic, due to the large water volume and the low nutrient availability (Wagner et al., 2010) with a surface water specific conductivity of ca. 200 $\mu S\,cm^{-1}$ and a pH of around 8.4 (Matter et al., 2010). The hydrological characteristics are mainly controlled by a relatively low water input of 37.9 $m^3\,s^{-1}$, of which ~ 50 % derives from karst aquifers (Matzinger et al., 2006a, b). The natural catchment area is relatively small with 1042 km^2 (Matzinger et al., 2006b; Wagner et al., 2008). Lake Ohrid is situated within the Lake Ohrid Basin, which is a 40 km long N–S trending graben structure in the Dinarides-Albanides-Hellenides mountain belt. The pull-apart like formation of the basin during a late phase of Alpine orogeny in the Miocene and the following subsidence led to the development of an early lake system (Reicherter et al., 2011). The exact age of the formation of the lake is still unknown and subject of several studies within the SCOPSCO project.

In the N and NE of the basin Palaeozoic metamorphic rocks crop out, which are superimposed by Triassic to Early Jurassic karstified platform carbonates (cf. Fig. 1b) in the E, NW and at the up to 2300 m a.s.l. high Galicica Mountains in the SE (Robertson and Shallo, 2000). Jurassic ophiolites and Tertian conglomerates form the Mocra Mountains of the SW graben shoulder (Robertson and Shallo, 2000). Mesozoic intru-

BGD
12, 15411–15460, 2015

sions of rhyolites and diabases are preserved in between the limestones and dolomites in the NE locally (Hoffmann et al., 2010). Within this geological setting the youngest active volcanism is reported for Early to Middle Miocene times, when volcanism occurred in central and eastern Macedonia due to extension in the Vardar zone and the Serbo-Macedonian massif. The occurrence of a hydrothermal field near Kosel in the north of the basin is most likely fault related since no other hints for volcanic activity in younger times have been found during detailed field mapping (Reicherter et al., 2011). The plains in the N and S of Lake Ohrid are covered with lacustrine and alluvial plain sediments of Quaternary age (Watzin et al., 2002).

3 Material and methods

During an ICDP deep drilling campaign at Lake Ohrid in spring 2013 six parallel holes were drilled at the main drill site, the DEEP site (cf. Fig. 1b), down to a maximum sediment depth of 569 m below lake floor (b.l.f.). The coring location (40 m distance between the individual holes) can be averaged to 41°02′57′′ N and 20°42′54′′ E at a water depth of 243 m.

The cores of the DEEP site sequence were lengthwise opened, visual described, and subsequently scanned by X-ray fluorescence with an ITRAX core scanner (COX Ltd) at the University of Cologne. Based on the core description and the XRF data the uppermost 247.8 mcd of the DEEP site sequence were correlated to a composite profile (Francke et al., 2015). The core halves were visually screened for conspicuous horizons showing changes in macroscopic grain size or colour to identify potential tephra layers. Smear slides of these horizons were then checked for the occurrence of glass shards and micro-pumices using a Leitz DM EP polarization microscope.

Once a tephra layer was identified, bulk samples were taken from the respective horizon and embedded in epoxy resin. The epoxy pucks were polished to avoid compositional variations due to topographic effects and carbon-coated to enable conductivity during the following SEM and EDS/WDS-analysis. A first screening of major element

BGD
12, 15411–15460, 2015

compositions of single glass shards and micro-pumice was done using a SEM Philips XL30 equipped with an energy dispersive spectroscope (EDS) EDAX DX4. Operating conditions were adjusted at 20 kV accelerating energy, 200–500 nm beam diameter, 9–10 A beam current, 100 s live time with 2100–2400 shots per second, and ZAF-correction (Z: atomic number; A: absorption; and F: fluorescence). The initial calibration, using four reference standards (albite, olivine and the glasses CFA47 and KE12), and the performance of the machine are described in detail by Marianelli and Sbrana (1998). In order to obtain more accurate quantitative analysis and to enlarge the comparability/reproducibility with existing datasets, a second screening of the samples was performed using the more common wavelength dispersive spectrometer (WDS) technique at the Istituto di Geologia Ambientale e Geoingegneria of the Italian National Research Council (IGAG-CNR, Rome). A Cameca SX50 electron microprobe equipped with a five wavelength dispersive spectrometer was set to the following operating conditions: 15 kV; beam current, 15 nA; beam diameter, 10–15 mm; and counting time 20 s per element. Wollastonite (Si and Ca), corundum (Al), diopside (Mg), andradite (Fe), rutile (Ti), orthoclase (K), jadeite (Na), phlogopite (F), potassium chloride (Cl), baritina (S), and metals (Mn) were used as standards. Titanium contents were corrected for the overlap of the Ti and K_α peaks. Two international secondary standards (Kanui augite and rhyolite RLS132 glasses, from the United States Geological Survey) were analysed prior sample measurements to evaluate the accuracy of the analyses. The mean analytical precision was < 1 % for SiO_2 and up to 1, 5, 15, 30, and > 50 % for all the elements in concentration range of > 15–30, > 5–15, > 1–5, < 1–> 0.3, and < 0.3 wt %, respectively.

All geochemical compositions were recalculated as being 100 % water-free. The geochemically classification of the composition of shards and micro-pumice was done with the total alkali vs. silica (TAS) diagram (Bas et al., 1986). Identified tephra layers are labelled unambiguously with the site name (OH-DP for Ohrid-DEEP) and the correlated bottom depth of each layer (e.g. “OH-DP-corr. depth in dm”).

BGD
12, 15411–15460, 2015

4 Results

The here presented uppermost 247.8 mcd of sediments from the DEEP site sequence mainly consist of fine-grained hemiplegic sediments with some intercalated more coarse-grained beds. A detailed lithological description and the discussion of sedimentological processes and paleoenvironmental information is given by Francke et al. (2015). Interglacial sediments indicate high amounts of calcite and organic matter, whereas glacial sediments are dominated by clastic, terrigenous components.

In total, 32 macroscopic tephra layers were identified in the upper 247.8 mcd of the DEEP site sequence (Fig. 2). Here, we present data of 12 macroscopic tephra layers, which could have been unambiguously correlated with known eruptions, and of one cryptotephra, which was already recognized in shorter cores of Lake Ohrid (Vogel et al., 2010; Wagner et al., 2012). A detailed geochemical description of the remaining tephra layers, which are not all analyzed and correlated with known eruptions at present, and a discussion of potential ages and origins will be given elsewhere, as it is beyond the scope of this paper. Thickness information is given for tephra layers only, because the cryptotephra did not form a visible horizon.

Cryptotephra OH-DP-0027 was recognized by correlating the XRF potassium curve of the DEEP site record with those of nearby core Co1262 (Wagner et al., 2012) and core Co1202 from the NE part of the lake (Vogel et al., 2010). In cores Co1262 and Co1202 a potassium peak is caused by the presence of glass shards of the cryptotephra OT0702-3 and Co1262-709. A similar peak is found in the DEEP site sequence at 2.773 mcd, and a more detailed inspection of this depth revealed also the occurrence of volcanic particles at this depth. The discovered volcanic particles of OH-DP-0027 are highly vesicular micro-pumices having spherical or elongated vesicles and glass shards with thick septa or a platy shape.

Tephra layer OH-DP-0115 (11.492–11.507 mcd) is 1.5 cm thick, brownish-greyish in colour and has sharp upper and lower boundaries. OH-DP-0115 comprises both highly vesicular micro-pumices with elongated vesicles and bubble-wall and -junction glass

BGD
12, 15411–15460, 2015

shards. The glass composition is mainly trachytic with a tendency towards the phonolitic field in the TAS-diagram (Fig. 3b, Table 1).

Tephra OH-DP-0169 (16.783–16.933 mcd) has a thickness of 15 cm, which makes it the thickest tephra layer within the so far studied DEEP site sequence. It can be visually separated in two units. The lower unit (OH-DP-0169a) has a sharp boundary at the bottom, is 2 cm thick and pale yellow in colour, whereas the upper unit (OH-DP-0169b) is 13 cm of pale brown, coarser material. The uppermost centimetres of the upper unit are mixed with lacustrine sediments and have an uneven top boundary, which is probably due to a difficult penetration during coring. Both units comprise elongated vesicle bearing micro-pumices, bubble-wall and -junction shards with thick septa, and have the same trachytic to phono-trachytic glass composition (Fig. 3c, Table 1).

Tephra layer OH-DP-0404 (40.456–40.486 mcd) is a 3 cm thick dark reddish brown horizon with sharp transitions at the top and bottom. The layer comprises elongated vesicular micro-pumices and thick walled bubble-wall shards. Glass composition analyses reveal a mainly phonolitic composition with some shards scattering around the intersection of tephriphonolitic, trachyandesitic, and trachytic fields in the TAS-diagram (Fig. 3d, Table 1).

Tephra OH-DP-0435 (43.498–43.513 mcd) is a 1.5 cm thick, greyish brown layer with sharp top and bottom contacts. The horizon comprises highly vesicular micro-pumices and bubble wall shards with thick septa, which mainly have a trachytic glass composition. However, some shards are also plotting in the phonolitic field of the TAS-diagram (Fig. 3e, Table 1).

The OH-DP-0499 (49.937–49.947 mcd) tephra layer is 1 cm thick, olive brown, and characterised by a sharp bottom and a diffuse top boundary. It comprises elongated vesicular micro-pumices and larger platy bubble wall shards. The glass composition is bimodal with a distinctly separated trachytic and rhyolitic group (Fig. 3f, Table 1). According to the Al_2O_3-FeO_{TOT} diagram (Fig. 4), glass shards have a mainly pantelleritic composition with some shards plotting in the comenditic field.

BGD
12, 15411–15460, 2015

Title Page
Abstract Introduction
Conclusions References
Tables Figures
◀◀ ▶▶
◀ ▶
Back Close
Full Screen / Esc
Printer-friendly Version
Interactive Discussion

The tephra layer OH-DP-0617 (61.701–61.726 mcd) is a yellowish brown, 2.5 cm thick deposit with sharp bottom and top contacts. The very fine-grained glass shards have various forms, being highly vesicular with circular and oval bubbles. Micro-pumices with elongated vesicles are rare. The chemical glass composition is a homogenous phonolite (Fig. 3f, Table 1).

Tephra OH-DP-0624 (62.367–62.413 mcd) is 4.6 cm thick, of olive brown colour and has a sharp bottom and more diffuse top transition. It comprises micro-pumices with elongated vesicles, cuspate glass shards, and non-vesicular, blocky, porphyric particles, bearing prismatic microlites and phenocrysts. In the uppermost diffuse part, volcanic fragments are mixed with authigenic siderite crystals. The glass composition spans from the phonotephritic to the phonolitic field of the TAS-diagram (Fig. 3g, Table 1).

Tephra layer OH-DP-1817 (181.744–181.769 mcd) is a dark brownish layer with a thickness of 2.5 cm and sharp bottom and top contacts. The layer contains mostly non-vesicular, blocky porphyric shards with a high content of microlites and phenocrysts. Vesicular cuspate shards are rare and are also porphyritic. The composition is low evolved plotting in the foiditic field of the TAS-diagram (Fig. 3h, Table 1).

The tephra layer OH-DP-1955 (195.536–195.566 mcd) is 3 cm thick and has a sharp bottom and a diffuse top boundary. The greyish layer comprises blocky, non-vesicular glass shards and porphyric micro-pumices containing leucite crystals. The composition is mainly phonolitic to trachy-andesitic with some shards plotting in the tephri-phonolitic field (Fig. 3h, Table 1).

OH-DP-2010 (201.034–201.049 mcd) is a reddish-brown, 1.5 cm thick layer with a sharp lower and an undulated upper boundary. It comprises morphological different volcanic fragments, which range from non-vesicular, microlite-bearing blocky, glass shards, to medium vesicular cuspate glass shards, and elongated vesicular micro-pumices. The TAS-diagram shows a characteristic tephriphonolitic to phonolitic composition (Fig. 3i, Table 1).

BGD
12, 15411–15460, 2015

Tephra layer OH-DP-2017 (201.747–201.782 mcd) is whitish to yellowish, 3.5 cm thick, and has sharp bottom and top boundaries. The horizon contains highly vesicular cuspate glass shards with a varying morphology and septa thickness. The chemical glass composition is homogenous trachytic (Fig. 3j, Table 1).

Tephra OH-DP-2060 (206.060–206.080 mcd) is a 2 cm thick, brownish-greyish tephra layer with a sharp bottom and a more diffuse upper boundary. The layer comprises mainly non-vesicular, porphyritic (leucite and sanidine), blocky glass shards. Furthermore, numerous diatoms and weathered calcite were found during microscope analysis. The composition is mainly foiditic (Fig. 3j, Table 1).

5 Discussion

A primary origin of the tephra layers from the direct surrounding of Lake Ohrid is highly unlikely, as there is no volcanic activity recorded for the Quaternary. Potential volcanic sources within the Mediterranean area are the Italian Provinces, the Hellenic Arc, or the Anatolian provinces. Pyroclastic deposits from the Hellenic Arc and the Anatolian Provinces are mainly calc-alkaline, often have very high silica contents, were primarily dispersed in eastern directions (Druitt et al., 1995, 1999; Aksu et al., 2008; Hamann et al., 2010; Sulpizio et al., 2013; Sumita and Schmincke, 2013; Keller et al., 2014; Tomlinson et al., 2015), and have not been found so far in the sediment records of Lake Ohrid (Sulpizio et al., 2010) and nearby Lake Prespa (Damaschke et al., 2013). Furthermore, they were not found in the numerous tephrological studies from the Tyrrhenian, Adriatic or Western Ionian Sea.

Mainly eastern distribution is also assumed for Italian tephra layers, and some of them were even found in the Eastern Mediterranean and Aegean Sea (Margari et al., 2007; Sulpizio et al., 2010; Karkanas et al., 2015; Satow et al., 2015).

All tephra discussed here show an alkaline affinity, which is only known from the Italian Volcanic Provinces in the Mediterranean region (Peccerillo, 2005). The existing records from Lakes Ohrid and Prespa contain tephra, only from Italian volcanoes,

BGD
12, 15411–15460, 2015

which were transported by the prevailing westerlies with E–SE direction in the upper atmospheric wind system. The Quaternary Italian volcanism is classified in several magmatic provinces (Washington, 1906; Peccerillo, 2005), which are mainly located along the Tyrrhenian coast of the Italian Peninsula, in the Tyrrhenian Sea, and in the Sicily channel, between 500 and 1000 km apart of Lake Ohrid (Fig. 1). In the studied succession (< 640 ka) explosive volcanic activity of Italian volcanoes is known so far from the Roman Province (Vulsini, Vico, Sabatini, Colli Albani), the Ernici-Roccamonfina area (Mt. Ernici, Roccamonfina), the Campania Province (Somma-Vesuvio, Campi Flegrei, Procida, Ischia), the Pontine Islands (Ventotene. Santo Stefano), the Mount Vulture, the Aeolian Arc (Alicudi, Filicudi, Salina, Lipari, Vulcano, Panarea, Stromboli) and the Sicily Province (Mt. Etna, Ustica, Pantelleria) (Fig. 1, Peccerillo, 2005).

The products of these Italian volcanoes span a wide compositional field ranging from subalkaline to alkaline and from mafic to silicic, depending on their geodynamic setting or mantle source (Lustrino et al., 2011). Most of them have a potassium or a high-potassium affinity (Roman, Roccamonfina, Campanian, and Pontine Islands) and their large chemical similarity or overlap in composition makes tephrostratigraphic work very challenging (Sulpizio et al., 2010). An origin from one of these provinces is supposed by the (high) alkaline phonolitic and trachytic compositions of most of the tephra layers found in the DEEP site sequence. However, some of the tephra layers in the DEEP site succession show more specific and unique compositions, which allow more straightforward correlations to the Pantelleria Islands and Somma-Vesuvius (Peccerillo, 2005), or the silica undersaturated, low evolved pyroclastic products of Colli Albani (Giaccio et al., 2013a).

5.1 OH-DP-0027/Mercato

The stratigraphic position and the occurrence of glass shards allow a correlation of OH-DP-0027 with the cryptotephras OT0701-3 (Vogel et al., 2010) and Co1262-709 (Wagner et al., 2012) from Lake Ohrid and PT0915-2 from Lake Prespa (Damaschke et al., 2013) and thus the correlation with the Pomici di Mercato (PdM) eruption from the Somma-Vesuvius volcano (cf. Fig. 3a).

The products of the PdM eruption are found as two distinct layers TM6a and TM6b in the Lago Grande di Monticchio record (Wulf et al., 2004). The double layers has been interpreted as due to shortly interrupted eruptive phases of the eruption (Mele et al., 2011). OH-DP-0027 matches better with TM6b, which represents the main Plinian and initial phase of the eruption (Wulf et al., 2004). A correlation with the PdM eruption is also established for a tephra found in the Veliko Jezero on the Island of Mljet (Croatia), where even several eruptive phases are indicated (Jahns and van den Bogaard, 1998). Also in sediment cores from the Adriatic Sea, such as the KET8218 (Paterne et al., 1988), IN68-9, IN68-5 and RF95-11 (Calanchi and Dinelli, 2008), or AD91-17 (Marchini et al., 2014), or from the Northern Ionian Sea MD90-918 210/223 (Caron et al., 2012) tephra layers were correlated with the PdM eruption.

Santacroce et al. (2008) reviewed several existing ^{14}C ages on proximal deposits of the Mercato eruption and suggested a maximum age of 9010–8750 cal a BP. This age is somewhat younger than the varve age obtained from the Lago Grande di Monticchio record for TM6b (9680 ± 480 cal a BP; Wulf et al., 2004). The most reliable age of 8630–8430 cal a BP comes probably from ^{14}C dating of charcoals collected at the basal part of the proximal fallout deposit Zanchetta et al. (2011).

5.2 OH-DP-0115/Y-3

The distinct trachytic composition of OH-DP-0115 suggests a correlation with the prominent marine tephra layer Y-3 from the Campanian area (Keller et al., 1978; Albert et al., 2015). The slightly heterogeneous major element composition, with a low and a high silica end-member is defined by Albert et al. (2015) as the diagnostic characteristic of the Y-3 tephra and perfectly matches the OH-DP-0115 tephra (cf. Fig. 3b). The Campi Flegrei (CF) caldera is as the most probable source of Y-3 (Di Vito et al., 2008; Zanchetta et al., 2008; Albert et al., 2015), but to date none of the suggested proximal counterparts, indicating a specific eruption, could be unambiguously assigned as its

BGD
12, 15411–15460, 2015

origin (Albert et al., 2015). Furthermore, the former most accepted correlation of the Y-3 with the intracaldera VRa and the mid-distal SMP1e/CE1 deposits (Sulpizio et al., 2003; Di Vito et al., 2008) is rejected in the light of new geochemical data separating the Y-3 from other CF eruptions of the Tufi Biancastri/NYT series (Tomlinson et al., 2012; Albert et al., 2015).

The Y-3 tephra is known as a widespread stratigraphic marker found in different archives in the Central and Eastern Mediterranean region, such as the Lago Grande di Monticchio (TM15, Wulf et al., 2004; Tomlinson et al., 2012), the Southern Adriatic Sea (MD90-917, Zanchetta et al., 2008), Lake Ohrid (0T0520-2; OT0700-1; OT0702-4; JO 187, summarized in Sulpizio et al., 2010), Lake Prespa (PT0704-1, Damaschke et al., 2013), and the Tenaghi Philippon peat record in Greece (TP 9.70, Albert et al., 2015). These correlations are validated by the low and high silica end-member (Albert et al., 2015). The correlations of the marine tephra layers C-7 (Paterne et al., 1988; Zanchetta et al., 2008), A2/B2 (Munno and Petrosino, 2004), and the terrestrial S19 layer (Munno and Petrosino, 2007) with the Y-3 tephra were not revaluated by Albert et al. (2015) due to restricted data sets, but seem to be likely.

Since no proximal equivalents could be unambiguously identified so far, the ages from these proximal correlations (e.g., 31–30 ka cal BP, Zanchetta et al., 2008) have to be rejected (Albert et al., 2015). However, a Bayesian age-depth model based on multiple radiocarbon ages above and below the TP 9.70 tephra of the Tenaghi Phillipon record provides an age of 28.68–29.42 cal ka BP (Albert et al., 2015). This is probably the best age, which is supported by radiocarbon ages from other distal archives, for example the ^{14}C-age of 28.78–29.98 ka cal BP obtained at the top of the Ohrid tephra OT07042-4/Y-3 (Vogel et al., 2010). The Y-3 tephra represents an important marker in the Mediterranean area, linking marine and terrestrial archives close to the Marine Isotope Stage 3/2 transition and the North Atlantic Heinrich Stadial 3 (HS3).

BGD
12, 15411–15460, 2015

5.3 OH-DP-0169/Y-5 CI

The characteristic trachytic to phonotrachytic alkaline composition of OH-DP-0169 (cf. Fig. 3c) and its remarkable thickness allow an unambiguous correlation with the Campanian Ignimbrite (CI) eruption (Orsi et al., 1996; Civetta et al., 1997; Pappalardo et al., 2002) and the marine tephra layer Y-5 (Keller et al., 1978; Thunell et al., 1979).

The deposits of the CI have a trimodal composition due to a strongly zoned, two layered trachytic magma chamber, whose distinct evolved products were tapped during different phases of the eruption and their interaction probably produced a third intermediate composition (Civetta et al., 1997; Pappalardo et al., 2002; Marianelli et al., 2006). According to Civetta et al. (1997) the largest part of OH-DP-0169 belongs to the most evolved composition (K_2O/N_2O 1.1–1.35) and only some shards can be assigned to the intermediate group (K_2O/N_2O 1.37–1.42). As the two parts of OH-DP-0169 (a+b) cannot be geochemically discriminated, the initial Plinian phase (cf. Marianelli et al., 2006) may correspond with the lower, pale yellow and more fine-grained part (OH-DP-0169a), while the main ignimbrite phase probably corresponds with the upper, pale brown and coarser part (OH-DP-0169b).

The CI/Y-5 tephra layer, originating from the Campi Flegrei (e.g. Pappalardo et al., 2002), is the most widely dispersed tephra marker in the Mediterranean region. It was found, for example, in sediment cores from the Lago Grande di Monticchio (TM-18, Wulf et al., 2004), the Greek island of Lesvos (ML 2, Margari et al., 2007), the Tyrrhenian Sea (C-13, Paterne et al., 1988; Ton-That et al., 2001) and in previous studies at Lake Ohrid (OT0520-3; OT0700-2; OT0701-1; OT0702-6; JO-244, summarized in Sulpizio et al., 2010) and Lake Prespa (PT0704-3, Damaschke et al., 2013). To date, the most distal finding is in the Russian Plain, 2500 km away from its source (Pyle et al., 2006).

The ages for the CI cluster around 40 ka. The varve chronology of Lago Grande di Monticchio yielded an age of 36.77 cal ka BP (Wulf et al., 2006). $^{40}Ar/^{39}Ar$ dating on single sanidine crystals revealed ages of 37.1 ± 0.4 ka (Deino et al., 1994), $41.1 \pm$

BGD
12, 15411–15460, 2015
First tephrostratigraphic results of the DEEP site record
N. Leicher et al.

2.1 ka (Ton-That et al., 2001) and 39.28 ± 0.11 ka (De Vivo et al., 2001), with the latter regarded as the best age, as it derives from proximal deposits.

5.4 OH-DP-0404/TM24a POP2

Tephra OH-DP-0404 has a similar, somewhat more variable phonolitic composition as tephra OT-0702-8 (cf. Fig. 3d), found in Ohrid core Co1202 (Vogel et al., 2010), which was correlated with the Monticchio tephra TM24a (Wulf et al., 2004, 2012). The TM24a tephra was first correlated with the prominent marine X-5 layer (Keller et al., 1978), but this correlation was later revised and the older Monticchio tephra TM25 was correlated with the X-5 layer (Wulf et al., 2012). The proximal or the marine tephra counterparts of TM24a remain unknown so far. OH-DP-0404 can be further correlated with the recently found POP2 tephra in the Popoli section from the Sulmona basin, which is also correlated with the TM24a tephra (Regattieri et al., 2015). A potential correlation of OH-DP-0404 with marine tephra layers from core CM92-42 (710 cm) and core RF93-77 (797 cm), which were also correlated with the TM24 (Calanchi and Dinelli, 2008), is likely, however, there is no differentiation between the bifurcation of tephra TM24 (a+b) in these marine tephras. According to the Monticchio varve record, TM24a has an age of 101.8 ± 5 ka (Wulf et al., 2012), which matches very well the age of 102.0 ± 2.4 ka obtained from the age-model of the Sulmona basin (Regattieri et al., 2015).

5.5 OH-DP-0435/X-6

The low alkali ratio (LAR) trachytic glass composition with only few shards plotting in the phonolitic field and its position below OH-DP-0404/TM24a/POP2 suggest a correlation of OH-DP-0435 with the marine tephra layer X-6 (Keller et al., 1978). The correlation is supported by the geochemically similarity of OH-DP-0435 with the Ohrid tephras OT0702-9 (Vogel et al., 2010) and JO-575 (Caron et al., 2010), which were also correlated with the X-6 layer (cf. Fig. 3e). Equivalents of the X-6 tephra are also found in marine cores of the Tyrrhenian Sea (C-31, Paterne et al., 2008; t1, Iorio et al., 2014) the Adriatic Sea (PRAD-2812, Bourne et al., 2015), and the southern Ionian Sea (I-9, Insinga et al., 2014). Furthermore, the X-6 is known from the terrestrial records of the Lago Grande di Monticchio (TM27, Wulf et al., 2012), the San Gregorio Magno basin (S10, Munno and Petrosino, 2007), the Cilento coastline (SM1-2/SA, Marciano et al., 2008; CIL2, Giaccio et al., 2012), and the Popoli section of the Sulmona basin (POP4, Regattieri et al., 2015). The origin of the X-6 is assigned to an unknown eruption of the Campanian area (Keller et al., 1978; Paterne et al., 2008; Wulf et al., 2012).

Based on $^{40}Ar/^{39}Ar$ dating, the age of tephra layer X-6 is 107 ± 2 ka (Kraml, 1997), which fits to the varve-based age of ca. 108.3 ± 5.4 ka BP of the TM-27 layer in Lago Grande di Monticchio (Wulf et al., 2012) and the interpolated age of 107 ka of the C-21 tephra layer (Paterne et al., 2008). More recently, a $^{40}Ar/^{39}Ar$ age of 108.9 ± 1.8 ka was obtained on deposits of the Cilento offshore area (t1 tephra, Iorio et al., 2014), which matches well the interpolated age of the Popoli section (109.0 ± 1.5 ka, Regattieri et al., 2015).

5.6 OH-DP-0499/P-11

OH-DP-0499 has a distinct bimodal chemical composition, with a clearly separated trachytic and a rhyolitic group. The shards can be classified as comendites and pantellerites (cf. Al_2O_3-FeO_{TOT} diagram Fig. 4), which unambiguously assigns them to an origin from the Pantelleria Island, the only source of these type of magmas in the Mediterranean region (Peccerillo, 2005). The twofold composition is explained by a chemically zoned magma chamber, in which peralkaline rocks originating from mantle-derived parental magma and trachytic magma differentiated in a low-pressure magma chamber by crystal-liquid fractionation (Civetta et al., 1984).

The stratigraphic position of OH-DP-0499, below the X-6 tephra (OH-DP-0435), infers a definite correlation with the P-11 tephra (cf. Fig. 3f) found in the Ionian Sea core KET82-22 (Paterne et al., 2008), since other widespread eruptions of the Pantelleria Island are much younger (ca. 77 ka, P-10, Paterne et al., 2008; 45.7 ka, Green Tuff, Scaillet et al., 2013). Furthermore, the geochemical fingerprint of OH-DP-0499 is identical to those of the two cryptotephras OT0702-10 (Vogel et al., 2010) and JO-941 (Caron et al., 2010) found previously in Lake Ohrid sediments and which were correlated with the P-11. A more proximal core from the Sicily Channel (ODP 963A) comprises three pantelleritic layers (ODP2-4) in a similar stratigraphic position (Tamburrino et al., 2012). ODP2 shows a somewhat different geochemical composition (benmoritic part) compared to OH-DP-0499/P-11. ODP3 and ODP4 indicate a very similar composition, but ODP3 is formed as a distinct horizon, whereas ODP4 is a cryptotephra (Tamburrino et al., 2012). Due to chronological concerns, Tamburrino et al. (2012) correlated ODP3 with the P-11, which is supported by their climastratographic position at the transition from MIS 6 to 5 (cf. Zanchetta et al., 2015). As only one pantelleritic layer is found in distal archives, ODP2 was precluded due to chemical considerations, ODP4 is a cryptotephra, and a correlation of ODP3 with the P-11 layer is the most likely and supposes that this tephra is the most widespread.

OH-DP-0499 can be further correlated with the ML5 tephra found on Lesovs Island (Margari et al., 2007), as already suggested by Vogel et al. (2010) for the OT0702-10 tephra. The ML5 tephra was previously correlated with the younger Green Tuff/Y-6, but the geochemical data support a correlation with the older P-11 tephra. In more recent studies, Karkanas et al. (2015) correlated a pantelleritic cryptotephra (THP-TII5) found in the Theopetra cave in central Greece with the P-11 and its equivalents. Satow et al. (2015) found a cryptotephra (LC21 10.345) in the Aegean Sea core LC21, which he ascribed to one of the ODP2-4 tephras. The position of LC21 10.345 in the *G. ruber* δ^{18}O record of LC21 implies a correlation with ODP3 and P-11 based on the position in the respective isotope records. Nevertheless, it has to be stated that only the rhyolitic endmember of P-11 was found in the records from LC21 and Theopetra. The typical comenditic trachytic part is not found in these archives, which is probably due to a different dispersal of the twofold zonation of the magma chamber (rhyolitic/trachytic part) tapped at different phases of the eruption. This is also indicated by an internal zonation of the OPD3 layer. Whereas the bottom of ODP3 has a pantelleritic composition, its top comenditic trachytic compositions (Tamburrino et al., 2012). This suggests that the rhyolitic pantelleritic part was erupted first and dispersed over a larger area, while the comenditic trachytic part is distributed only in a smaller, northern sector. Changes of the plume direction and dispersal during an eruption are likely due to changes in the aerodynamic characteristics of the erupted material or in the high and low atmosphere dynamics (Sulpizio et al., 2008, 2013).

The age-depth model of core KET82-22, based on orbital tuning of the oxygen isotope and sapropel stratigraphy, provided an age of 130.6 ± 5 ka for the P-11 tephra (Paterne et al., 2008). This age matches well the age of 128.1 ka of ODP3, which is inferred from correlation of benthic and planktonic foraminifera $\delta^{18}O$ curves of core ODP-963A with the SPECMAP stack curve (Incarbona et al., 2008; Tamburrino et al., 2012). The tentative correlation of LC21 10.345 with P-11 provides an age of 133.5 ± 2 ka, based on the correlation of the surface-water foraminiferal $\delta^{18}O$ record of LC21 to the U/Th dated Soreq Cave $\delta^{18}O$ record (Grant et al., 2012).

Proximal counterparts of the P-11 are the ignimbrite deposits of the P-unit on Pantelleria Island (Mahood and Hildreth, 1986; Paterne et al., 2008; Tamburrino et al., 2012). These proximal P-unit deposits provided $^{40}Ar/^{39}Ar$ ages between 123 ± 1.6 ka and 135 ± 1.2 ka, with a mean age of 129 ± 5.9 ka (Rotolo et al., 2013) and are in good accordance with the non-radiometric ages from the distal deposits.

5.7 OH-DP-0617/Vico “Ignimbrite B”

The characteristic homogenous phonolitic composition of OH-DP-0617 is very similar to the composition of tephra OT0701-6 (cf. Fig. 3f), which was found in the Ohrid core Co1201 (Sulpizio et al., 2010). OT0701-6 was previously correlated with the marine tephras C-20 and the proximal deposits of the SA3-b eruption from the Campanian area (Sulpizio et al., 2010). However, the correlation of C-20 with OH-DP-0404 and the stratigraphic position of OH-DP-0617 below the X-6/OH-DP-0435 and P11/OH-DP-0499 tephra suggest that and OH-DP-0617 and OT0706-1 rather correlate with the CF-V4 tephra from the Campo Felice Basin (Giraudi et al., 2011). The CF-V4 tephra is correlated with the “Ignimbrite B” of the Vico volcano (Vico B, Ronciglione Formation,

BGD
12, 15411–15460, 2015

Bear et al., 2009), which also has a large geochemical similarity to the Ohrid tephras OH-DP-0617/OT0701-6. So far equivalents of this Vico eruption were not found in other archives. Laurenzi and Villa (1987) $^{40}Ar/^{39}Ar$ dated the Ignimbrite B on proximal deposits to 157 ± 3 ka.

5.8 OH-DP-0624/CF-V5/PRAD3225

OH-DP-0624 is characterised by a wide spectrum in composition ranging from phonotephritic to phonolitic. This characteristic is also observed for tephra OT0701-7 in core Co1201 from Lake Ohrid (Sulpizio et al., 2010). OT0701-7 was first subdivided into three different chemical groups (a-b-c), of which OT0701-7b tentatively was correlated with the tephra layer OT0702-8/TM24a/X-5 (Sulpizio et al., 2010). However, this correlation is not supported by the stratigraphic position of OT0701-7 below OT0701-6, as the latter correlates well with OH-DP-0617. Furthermore, OT0702-8/TM24a is correlated with OH-DP-0404, which is embedded by sediments of interglacial MIS5, whereas glacial sediments encompass OT0701-7 (Sulpizio et al., 2010). Also the glass composition of OT0701-7, showing a geochemical trend rather than different geochemical populations, makes a correlation with OH-DP-0624 more likely.

The very characteristic geochemical trend of OH-DP-0624 (cf. Fig. 3g) matches the marine tephra PRAD3225 from the Adriatic Sea (Bourne et al., 2015), which is tentatively correlated with the tephra 322 from core RF95-7 and with the TM38 in the Lago Grande di Monticchio record (Wulf et al., 2012). Tephra 322 was assigned to the Vico D eruption (Calanchi and Dinelli, 2008), which is dated to ca. 138 ka (Laurenzi and Villa, 1987). TM38 has an age of 125.6± 6.3 ka according to the varve chronology of the Lago Grande di Monticchio record (Wulf et al., 2012). The ages of TM38 and 322/Vico D are significantly too young for the stratigraphic position of OH-DP-0624 below the OH-DP-0617/Vico B and dated to ca. 157 ± 3 ka. Another marine counterpart of OH-DP-0624 could be tephra C-42 with its phonotephritic composition (Paterne et al., 2008), but the published average values do not allow a robust correlation.

BGD
12, 15411–15460, 2015

The most reliable equivalent of OH-DP-6024/OT0701-7/PRAD3225 is probably found in the Campo Felice basin in the Apennine chain. The geochemical composition and the stratigraphic position of the CF-V5 tephra, which was found in this basin directly below the CF-V4 tephra (Giraudi and Giaccio, 2015) correlates well with the composition and stratigraphic position of the OH-DP-6024 directly below the OH-DP-0617 tephra. Giraudi and Giaccio (2015) tentatively suggest that the CF-V5 tephra is an equivalent of the Pitigliano Tuff from the Latera caldera in the Vulsini volcanic complex (Turbeville, 1992a). Although the geochemical dataset is limited, a similar characteristic trend is observed in CF-V5 and OH-DP-0624/OT071-7. $^{40}Ar/^{39}Ar$ dating on proximal deposits of the Pitigliano Tuff provided ages of 158 ± 11 ka and 155 ± 11 ka (Turbeville, 1992a, b) and the overlying Vico Ignimbrite B tephra limits the minimum age to 157 ± 3 ka.

5.9 OH-DP-1817/Pozzolane Rosse

OH-DP-1817 has a K-foiditic composition, which is only known from the Italian volcanoes of the Colli Albani volcanic district (Peccerillo, 2005). The most widespread eruption from Colli Albani are the products of the Pozzolane Rosse eruption cycle (Giaccio et al., 2013a) of the Tuscalano-Aretemsio (T-A) phase in the Middle Pleistocene (Marra et al., 2011).

A correlation of OH-DP-1817 with proximal data of the Pozzolane Rosse eruption is difficult. Marra et al. (2009) describe the proximal type localities of the Pozzolane Rosse pyroclastic products, but only the mean value of one geochemical analysis is published (AH-20-PRa). Another, more comprehensive data set was obtained in modern quarry sections adjacent to the Colli Albani (Marra et al., 2011), but the tephra was strongly altered by weathering (e.g. high loss on ignition values, low totals due to loss of alkalis) and the XRF data cannot be directly compared to our EDS data. Therefore, the correlation OH-DP-1817/Pozzolane Rosse (cf. Fig. 3h) is mainly based on the data of the distal equivalents of the Pozzolane Rosse units, which are found in Paganica-San Demetrio-Castelnuovo and in the Sulmona basin in the Apennine chain, east of Colli

Albani (Galli et al., 2010; Giaccio et al., 2013a). Giaccio et al. (2013a) separates the Pozzolane Rosse distal equivalents into two sublayers, which differ chemically and morphologically. Most of the shards of OH-DP-1817 match the less evolved composition (group a) of the lower layer and only few analyses are prone to the more evolved composition (group b) of the upper sublayer cf. Fig. 3h). Besides the chemical correlation, microtextural features, such as the scoria character (dense, few vesicles) of the shards and the huge number of juvenile crystals observed in OH-DP-1817, support a correlation with the lower layer. Giaccio et al. (2013a) correlate the lower sublayer (group a) to the proximal Pozzolane Rosse basal fall-out and the upper sublayer to the phoenix cloud of the main pyroclastic flow-forming phase. According to Freda et al. (2011) the Pozzolane Rosse eruption sequence encompasses from bottom to top the Vallerano lava flow, the main Pozzolane Rosse pyroclastic units (basal fallout and main pyroclastic flow unit) and the scoria lapilli fallout deposits. Thus, most of the material of the tephra layer OH-DP-1811 can be assigned to the basal fallout of the Pozzolane Rosse eruption. Recently, the products of the Pozzolane Rosse eruption were also found in the Campo Felice basin and correlated with tephra layer CF-V11 (Giraudi and Giaccio, 2015).

The age of the Pozzolane Rosse eruption is well constrained by several $^{40}Ar/^{39}Ar$-ages. The pyroclastic products are dated to 457 ± 4 ka at a proximal site (Karner et al., 2001), which is confirmed by the distal equivalent found in the Sulmona Basin (457 ± 4 ka, Giaccio et al., 2013a). These ages are further framed and supported by $^{40}Ar/^{39}Ar$-ages of 457 ± 5 ka from a lava flow below and of 442 ± 2 ka from a relatively thin succession of fall out deposits on top (Marra et al., 2009).

5.10 OH-DP-1955/SC5

According to the stratigraphic position, OH-DP-1955 was deposited around or prior to ca. 450 ka. Proximal deposits of the active volcanoes in Italy older than 450 ka are only barely explored. From the more distal archives, the tephra layer SC5 from the Mercure Basin (Giaccio et al., 2014) shows a trachy-andesitic to phonolitic trend similar to that of OH-DP-1955 (cf. Fig. 3h). Investigated sources for OH-DP-1955 and its potential equivalent SC5 are very limited. Sr-isotope ratios of tephra layer SC5 reveal an origin from the Roccamonfina volcano (Giaccio et al., 2014). $^{40}Ar/^{39}Ar$ dating provided an age of 493.1 ± 10.9 ka for the SC5 tephra (Giaccio et al., 2014), which thus represents an unknown eruption from the Roccamonfina volcano, as the oldest known eruption is the Rio Rava eruption dated to 439 ka (Rouchon et al., 2008). A potential correlation of OH-DP-1955 with Fall B from the Tuffi Terrosi Eruptive Cycle from the Sabatini volcanic field despite a similar age is unlikely due to the geochemical difference between the tephras (cf., Sottili et al., 2004; Marra et al., 2014).

5.11 OH-DP-2010/Fall A

The tephri-phonolitic to phonolitic composition of tephra OH-DP-2010 and its characteristic high potassium content suggest an origin from the Roman province. The low Cl content of OH-DP-2010 (cf. Table 1) is typical for Middle Pleistocene Sabatini products (Giaccio et al., 2014) and supports an origin from the Tufi Terrosi Eruptive Cycle of the Sabatini volcanic district (Marra et al., 2014). The major element composition and the stratigraphic position suggest that OH-DP-2010 correlates with the proximal and distal products of the oldest eruptive unit Fall A (cf. Fig. 3i) of the Tufi Terrosi con Pomici Bianche (Karner et al., 2001; Sottili et al., 2004). The reddish colour of OH-DP-2010 can be attributed to the reddish, terracotta-like, thermally metamorphosed clay lithics, which are a diagnostic characteristic of the proximal Fall A deposits (Sottili et al., 2004). However, the proximal deposits of Fall A apparently show a smaller compositional range (cf. Marra et al., 2014) than in OH-DP-2010 and other distal archives, such as the Mercure Basin (SC3) and the Sulmona Basin (SUL 5-1c), whose correlation is corroborated by Sr-isotope analyses (Giaccio et al., 2014). Similar major element compositions suppose also a correlation of OH-DP-2010/Fall A with the Acerno tephra A9, whose origin has been unknown so far (Petrosino et al., 2014b).

Sottili et al. (2004) describe a bifurcation of the Fall A at the type section with a lower sublayer A1 and an upper sublayer A2 both comprising alternating layers of white pumice and grey scoria clasts. Whereas the white pumices of these eruptive units are more evolved and trachy-phonolitic, the grey scoria clasts have a phono-tephritic to tephri-phonolitic composition (Marra et al., 2014). The reason for the wider compositional spectrum of distal Fall A deposits (e.g. OH-DP-2010, SC3) could be the lack of data for the less evolved, upper grey pumices of the proximal zoned Fall A. A correlation of the older Grottarossa Pyroclastic Sequence (GPRS, Karner et al., 2001) of the Sabatini volcano (Marra et al., 2014) with the chemically similar and less evolved part of OH-DP-2010 can be excluded, since a paleosol separates the GPRS from Fall A in the type section (Sottili et al., 2004). Furthermore, the GPRS products and Fall A occur as two individual layers in the Sulmona Basin.

According to $^{40}Ar/^{39}Ar$ dating, the lower Fall A1 has an age of 499 ± 3 ka and the upper Fall A2 has an age of 496± 3 ka (Marra et al., 2014). However, unpublished age–depth interpolations from distal equivalents reveal slightly older ages, with 510± 3 ka for SC3 at the Mercure Basin, and with 502 ± 4 ka for the A9 at the Acerno Basin.

5.12 OH-DP-2017/A11/A12

The trachytic composition of OH-DP-2017 excludes an origin from Roman and Roccamonfina provinces, which mainly produced phonolites and tephro-phonolites during the Middle Pleistocene (cf. Giaccio et al., 2014). However, two very similar trachytic layers (A11/A12) are found in the Acerno Basin sequence (Petrosino et al., 2014b). They have a similar stratigraphic position and a similar glass chemical composition (cf. Fig. 3j) compared with OH-DP-2017 (Petrosino et al., 2014b). An unambiguous correlation of OH-DP-2017 with one of the both layers is not possible, due to their indistinguishable major element composition. Tephra SC2 from the Sulmona Basin was tentatively also correlated based on chemical affinities and its stratigraphic position with the A11/A12 (Giaccio et al., 2014). However, some differences in the composition do not support an unambiguous correlation of SC2 with OH-DP-2017 or A11/12 and suggest that they may derive from the same source, but from different eruptions.

BGD
12, 15411–15460, 2015

According to the geochemical characteristics, an origin of A11/12 from the Campanian area was proposed (Petrosino et al., 2014b). While proximal products of the Campanian area date back to ca. 290 ka only (Seiano Ignimbrite, Rolandi et al., 2003), distal deposits, such as the Montalbano Jonico succession (around 720 ka, V5, V7, Petrosino et al., 2015) and the Sulmona Basin (ca. 723 ka, SC1-35.30/SUL2-1, Giaccio et al., 2013b) suggest also older activity of the Campanian area, which may have produced OH-DP-2017/A11/A12. Although Sr-isotope ratios indicate that tephra layer SC2 originate from the Ponza Island, the lack of Middle Pleistocene pyroclastic rocks on Ponza Island contradicts this correlation and origin of SC2 from the Campanian area is more likely (Giaccio et al., 2014).

Sanidine crystals of the Acerno tephra A11 yielded a $^{40}Ar/^{39}Ar$ age of 514 ± 5.6 ka (Petrosino et al., 2014b). The stratigraphic distance of the Acerno layers A11 and A12 is 12 cm only, which amounts to an age difference of a few hundred years according to the sedimentation rate between the two tephra (Petrosino et al., 2014b). As this difference in age is negligible compared to the $^{40}Ar/^{39}Ar$ error of 5.6 ka, the age of 514 ± 5.6 ka can be transferred from the A11 to OH-DP-2017 tephra.

5.13 OH-DP-2060/Tufo di Bagni Albule

The characteristic K-foiditic composition of tephra layer OH-DP-2060 suggests an origin from the Colli Albani volcanic district. According to the stratigraphic position of OH-DP-2060 with a presumed age older than 510 ka, it can be assigned to the Tufo del Palatino-Tufo di Bagni Albule eruptive cycle of the Colli Albani volcanic district (Karner et al., 2001; Giaccio et al., 2013a). Glass composition data are only published for the upper pyroclastic flow Tufo di Bagni Albule (TBA or Tufo di Acque Albule), which is separated by a paleosol from the lower Tufo del Palatino (TP) ignimbrite (Marra et al., 2009). A geochemical comparison of the TBA with the proximal data of the Via Tiburtina section AH-23 (Marra et al., 2009) and the distal equivalent found in the Sulmona Basin (Giaccio et al., 2013a) reveals a good correlation with OH-DP-2060 (cf. Fig. 3j). A relatively thick, foiditic tephra with Tufo del Palatino-Tufo di Bagni Albule products was also found in a core from the Fucino basin in the Apennine chain (Giaccio et al., 2013a). In the Intra-Apennine Carsoli Basin, a chemically very similar deposit, the so-called the Oricola tuff was found (Stoppa et al., 2005) and later based on chronological, isotopic, and major element composition affinities correlated with TBA from the Colli Albani volcanic district (Giaccio et al., 2013a). The carbonate content of the Oricola tuff (Peccerillo, 2005; Stoppa et al., 2005), which is also noticed in OH-DP-2060, is typical for Colli Albani products, because the magma chambers are situated in Mesozoic limestones (Giordano et al., 2006).

TP and TBA in proximal deposits indicate geochronologically indistinguishable ages of 530 ± 2 and 527 ± 2 ka (Marra et al., 2009), which are in a good agreement with the age obtained for the Oricola tuff (ca. 531 ka, Bosi et al., 1991). As long as no compositional glass data is available for the TP, the TBA is the most likely equivalent of OH-DP-2060 and an age of 527 ± 2 ka can be assumed.

5.14 Recalculation and chronology of the DEEP site tephra layers

The obtained tephrochronological information from the dated equivalents of the DEEP site tephra layers were used to develop a robust chronology for the DEEP site sequence, for both the sediment core and the borehole sequence (cf. Baumgarten et al., 2015; Francke et al., 2015). For this purpose, 9 out of the presented 13 tephra layers were selected due to their radiometrically dated ages, except for the Y-3, where a high number of ^{14}C ages above and below allow a reliable age interpolation. In order to achieve a homogenous set of ages, all $^{40}Ar/^{39}Ar$ ages have been calculated based on the same flux standard (Fish Canyon sanidine (FCs) at 28.02 Ma and Alder Creek sanidine ACs-2, Nomade et al., 2005 and the total ^{40}K decay constant of Steiger and Jäger, 1977). This choice was made because most of the published ages were made using these two flux standards. Several calibrations of the $^{40}Ar/^{39}Ar$ chronometer are currently in use, which yield ages that vary by ∼ 1 % in the time range of the Pleistocene (e.g. Kuiper et al., 2008; Renne et al., 2010; Phillips and Matchan, 2013). As long as it is not the purpose of this work to decipher, which calibration is the more accurate and that the implied difference in calibrated age is within the current reported fully propagated uncertainties at 2σ level, we decided to keep ages as they were published without necessarily endorsing the flux standards values used. The results are indicted in Table 2.

Based on the 9 selected tephra layers, which are used as first order tie points, Francke et al. (2015) established an age-depth model including further 44 chronological tie-points for the uppermost 247.8 mcd of the DEEP site sequence. Second order tie points are tuned TOC and TOC related proxies (C/N) to local insolation and winter season length patterns (Laskar et al., 2004), third order tie points result from tuning, TIC maxima to LR04 minima (Lisiecki and Raymo, 2005). Finally, the established age-depth model was cross evaluated (logging K vs. composite core K) and fine-tuned with the age model of the borehole logging data (Baumgarten et al., 2015).

The ages of the tephra layers TM24a/POP2 were not considered in the recalculation (Table 2), because their ages were interpolated from the respective age-depth models and independent, radiometrically dated ages do not exist.

The age obtained from the suggested correlation OH-DP-0624/CF-V5 with the Pitigliano Tuff was recalculated, but not included in the age model, as the tephrostratigraphical correlation is not very robust (cf. discussion OH-DP-0624) and the 2σ error bar is relatively large (Table 2). Furthermore, the age of the directly overlying tephra OH-DP-0617/Vico B represents a more reliable tie-point in this part of the sequence. The tephra layers OH-DP-1955/SC5 and OH-DP-2060/Tufo di Bagni Albule were not included in the age-depth modelling, as the results of the geochemical analyses were not available when the age-depth model was established. The original/recalculated age of Fall A 499/496 ± 3 ka was not selected as a first order tie point for the age-depth model Francke et al. (this issue), since the age-depth interpolations of the Acerno Basin and the Mercure Basin suggest an older age for Fall A and the age of Fall A is questionable.

In order to obtain a first overview of the chronology of the DEEP site sequence, an age-depth plot (Fig. 5) with all tephrochronological information was created. The homogenous distribution of ages vs. depth suggests relatively constant sedimentation of the DEEP site sequence for the upper 247.8 m. Although the ages of OH-DP-0404/TM24a/POP2 and OH-DP-1955/SC5 were not included in the age model, they tentatively support to the age-depth curve (cf. Fig. 5).

As visualised in Fig. 5, the uncertainties of the $^{40}Ar/^{39}Ar$ age of Fall A (496 ± 3 ka) become more obvious. The tephra correlation OH-DP-1955/SC5 is located 5.48 m (2.9 ka) above OH-DP-2010/Fall A and OH-DP-2017/A11 is located 0.73 m (17.9 ka) below this layer. Accepting an age of 496 ± 3 ka for Fall A would imply a dramatic change in the sedimentation rates within this periods, with interpolated sedimentation rates (1.8 m ka^{-1} above and 0.04 m ka^{-1} below), which differ substantially from a mean sedimentation rate of 0.39 m ka^{-1} for the entire sequence. However, there is no lithological evidence for such a change in sedimentation. The radiometric dating of Fall A was done on deposits from Cava Rinaldi, which were correlated with Fall A only using trace element ratios (Zr/Y vs. Nb/Y plot) and chronological constraints, because the deposits have been too altered to use major element compositions (Marra et al., 2014). Although this method is helpful to distinguish between the different Italian provinces and between the different volcanic districts (Marra et al., 2011; Marra et al., 2014), it may be not suitable to distinguish between single eruptions, with similar composition. Moreover, the intense alteration of the deposits makes an unequivocal correlation difficult and the obtained age for Fall A probably too young. Following the correlation of OH-DP-2010 with distal deposits of the SC3 in the Mercure and the A9 in the Acerno basin, an age of between 502 and 510 ka seems to be more likely and would be consistent with more constant sedimentation rates in the DEEP site record.

6 Conclusions

First tephrostratigraphic studies on the DEEP site record from Lake Ohrid correlated 12 tephra layers and one cryptotephra with their counterparts, all originating from the Italian volcanism. The following correlations could be proposed: OH-DP-0027/Mercato tephra, OH-DP-0115/Y-3, OH-DP-0169/Y-5, OH-DP-0404/TM24a/POP2, OH-DP-

BGD
12, 15411–15460, 2015

0435/X-6, OH-DP-0499/P-11, OH-DP-0617/Vico "Ignimbrite B", OH-DP-0624/CF-V5/Pitigliano Tuff, OH-DP-1817/Pozzolane Rosse, OH-DP-1955/SC5, OH-DP-2010/Fall A, OH-DP-2017/A11/12, and OH-DP-2060/Tufo di Bagni Albule.

Tephra layers found in the previous studies could be re-identified and were helpful markers for developing the new tephrostratigraphy of the DEEP site record. The existing correlations could be emphasised and some of them corrected to the todays knowledge (e.g. OH-DP-0617/OT0701-6 and OH-DP-0624/OT0701-7). Furthermore, tephrostratigraphy was successfully applied for the sequence older than the already inspected 130 ka of Lake Ohrid's history. The Italian Middle Pleistocene tephrostratigraphic framework, which is based on several records covering specific intervals of time, was extended for the first time beyond Italy to the Balkan region and linked to an at least 640 ka old continuous record. This will provide a unique opportunity to achieve new results in stratigraphy, when the eruptive order of tephra layers found in different archives is unknown. Furthermore, this linkage and synchronization of different archives helps to find the origin of so far unknown tephra layers (e.g. OH-DP-2010/Acero tephra A9/Fall A) or improves suggested correlations (e.g. OH-DP-6024/CF-V5/PRAD3225). The connection to different records within the Mediterranean region reveals the possibility to review different distribution patterns of specific eruptions, which probably changed within an eruption (e.g. OH-DP-0499/P-11/THP-TII-5).

The recognition of tephras from volcanic provinces, which were thought to be inactive at the time of tephra deposition, such as the ca. 490 ka old OH-DP-1955/SC5 tephra from the Roccamonfina volcano, or the ca. 510 ka old OH-DP-2017/A11/12 tephra from the Campanian Volcanic Zone, improve our knowledge about volcanic activity of the different provinces. Furthermore, their widespread distribution to the Balkan suggest that some of them were rather large magnitude eruptions and represent widespread marker horizons.

The ages of 8 of the correlated tephra layers were used to contribute first order tie points to develop a robust age-depth model of the entire DEEP site sequence. This

BGD
12, 15411–15460, 2015

Title Page
Abstract Introduction
Conclusions References
Tables Figures
◀ ▶
Back Close
Full Screen / Esc
Printer-friendly Version
Interactive Discussion

age-depth model has the potential to improve our tephrochronological knowledge of some of the layers found in the Lake Ohrid sequence (e.g. Fall A, Pitigliano Tuff).

The Supplement related to this article is available online at doi:10.5194/bgd-12-15411-2015-supplement.

Acknowledgements. The SCOPSCO Lake Ohrid drilling campaign was funded by ICDP, the German Ministry of Higher Education and Research, the German Research Foundation, the University of Cologne, the British Geological Survey, the INGV and CNR (both Italy), and the governments of the republics of Macedonia (FYROM) and Albania. Logistic support was provided by the Hydrobiological Institute in Ohrid. Drilling was carried out by Drilling, Observation and Sampling of the Earth's Continental Crust's (DOSECC) and using the Deep Lake Drilling System (DLDS). Special thanks are due to Beau Marshall and the drilling team. Ali Skinner and Martin Melles provided immense help and advice during logistic preparation and the drilling operation.

References

Aksu, A. E., Jenner, G., Hiscott, R. N., and Isler, E. B.: Occurrence, stratigraphy and geochemistry of late quaternary tephra layers in the Aegean Sea and the Marmara Sea, Mar. Geol., 252, 174–192, 2008.

Albert, P. G., Hardiman, M., Keller, J., Tomlinson, E. L., Smith, V. C., Bourne, A. J., Wulf, S., Zanchetta, G., Sulpizio, R., Muller, U. C., Pross, J., Ottolini, L., Matthews, I. P., Blockley, S. P. E., and Menzies, M. A.: Revisiting the Y-3 tephrostratigraphic marker: a new diagnostic glass geochemistry, age estimate, and details on its climatostratigraphical context, Quaternary Sci. Rev., 118, 105–121, 2015.

Bas, M. J. L., Maitre, R. W. L., Streckeisen, A., and Zanettin, B.: A chemical classification of volcanic rocks based on the total alkali-silica diagram, J. Petrol., 27, 745–750, 1986.

Baumgarten, H., Wonik, T., Tanner, D. C., Francke, A., Wagner, B., Zanchetta, G., Sulpizio, R., Giaccio, B., and Nomade, S.: Age depth-model for the past 630 ka in Lake Ohrid (Mace-

donia/Albania) based on cyclostratigraphic analysis of downhole gamma ray data, Biogeosciences Discuss., 12, 7671–7703, doi:10.5194/bgd-12-7671-2015, 2015.
Bear, A. N., Cas, R. A. F., and Giordano, G.: Variations in eruptive style and depositional processes associated with explosive, phonolitic composition, caldera-forming eruptions: The 151 ka Sutri eruption, Vico Caldera, central Italy, J. Volcanol. Geoth. Res., 184, 225–255, 2009.
Bosi, C., Locardi, E., and Villa, I.: Il distretto magmatico abruzzese, Riassunti workshop "Evoluzione dei bacini Neogenici e loro rapporti con il magmatismo Plio-Quaternario nell'area Tosco-Laziale", Pisa 12–13 June 1991, 68–69, 1991.
Bourne, A. J., Albert, P. G., Matthews, I. P., Trincardi, F., Wulf, S., Asioli, A., Blockley, S. P. E., Keller, J., and Lowe, J. J.: Tephrochronology of core PRAD 1-2 from the Adriatic Sea: insights into Italian explosive volcanism for the period 200–80 ka, Quaternary Sci. Rev., 116, 28–43, 2015.
Calanchi, N. and Dinelli, E.: Tephrostratigraphy of the last 170 ka in sedimentary successions from the Adriatic Sea, J. Volcanol. Geoth. Res., 177, 81–95, 2008.
Calanchi, N., Cattaneo, A., Dinelli, E., Gasparotto, G., and Lucchini, F.: Tephra layers in late quaternary sediments of the central Adriatic Sea, Mar. Geol., 149, 191–209, 1998.
Caron, B., Sulpizio, R., Zanchetta, G., Siani, G., and Santacroce, R.: The Late Holocene to Pleistocene tephrostratigraphic record of Lake Ohrid (Albania), CR Geosci., 342, 453–466, 2010.
Caron, B., Siani, G., Sulpizio, R., Zanchetta, G., Paterne, M., Santacroce, R., Tema, E., and Zanella, E.: Late Pleistocene to Holocene tephrostratigraphic record from the Northern Ionian Sea, Mar. Geol., 311, 41–51, 2012.
Civetta, L., Cornette, Y., Crisci, G., Gillot, P. Y., Orsi, G., and Requejo, C. S.: Geology, Geochronology and Chemical Evolution of the Island of Pantelleria, Geol. Mag., 121, 541–562, 1984.
Civetta, L., Orsi, G., Pappalardo, L., Fisher, R. V., Heiken, G., and Ort, M.: Geochemical zoning, mingling, eruptive dynamics and depositional processes – The Campanian Ignimbrite, Campi Flegrei caldera, Italy, J. Volcanol. Geoth. Res., 75, 183–219, 1997.
Damaschke, M., Sulpizio, R., Zanchetta, G., Wagner, B., Böhm, A., Nowaczyk, N., Rethemeyer, J., and Hilgers, A.: Tephrostratigraphic studies on a sediment core from Lake Prespa in the Balkans, Clim. Past, 9, 267–287, doi:10.5194/cp-9-267-2013, 2013.

De Vivo, B., Rolandi, G., Gans, P. B., Calvert, A., Bohrson, W. A., Spera, F. J., and Belkin, H. E.: New constraints on the pyroclastic eruptive history of the Campanian volcanic Plain (Italy), Miner. Petrol., 73, 47–65, 2001.

Deino, A. L., Southon, J., Terrasi, F., Campajola, L., and Orsi, G.: ^{14}C and $^{40}Ar/^{39}Ar$ Dating of the Campanian Ignimbrite, Phlegran Fields, Italy, 8th International Conference on Geochronology, Cosmochronology and Isotope Geology, Berkeley, CA, USA, Abstracts US Geol. Surv. Circ., 1107, 77, 1994.

Di Vito, M. A., Sulpizio, R., Zanchetta, G., and D'Orazio, M.: The late Pleistocene pyroclastic deposits of the Campanian Plain: new insights into the explosive activity of Neapolitan volcanoes, J. Volcanol. Geoth. Res., 177, 19–48, 2008.

Druitt, T. H., Brenchley, P. J., Gokten, Y. E., and Francaviglia, V.: Late quaternary rhyolitic eruptions from the Acigol complex, Central Turkey, J. Geol. Soc. London, 152, 655–667, 1995.

Druitt, T. H., Edwards, L., Mellors, R., Pyle, D., Sparks, R., Lanphere, M., Davies, M., and Barreirio, B.: Santorini volcano, Geological Society, London, Memoirs, 19, 1–161, 1999.

Francke, A., Wagner, B., Just, J., Leicher, N., Gromig, R., Baumgarten, H., Vogel, H., Lacey, J. H., Sadori, L., Wonik, T., Leng, M. J., Zanchetta, G., Sulpizio, R., and Giaccio, B.: Sedimentological processes and environmental variability at Lake Ohrid (Macedonia, Albania) between 640 ka and present day, Biogeosciences Discuss., 12, 15111–15156, 2015, http://www.biogeosciences-discuss.net/12/15111/2015/.

Freda, C., Gaeta, M., Giaccio, B., Marra, F., Palladino, D. M., Scarlato, P., and Sottili, G.: CO_2-driven large mafic explosive eruptions: the Pozzolane Rosse case study from the Colli Albani Volcanic District (Italy), B. Volcanol., 73, 241–256, 2011.

Galli, P., Giaccio, B., and Messina, P.: The 2009 Central Italy earthquake seen through 0.5 Myr-long tectonic history of the L'Aquila faults system, Quaternary Sci. Rev., 29, 3768–3789, 2010.

Giaccio, B., Nomade, S., Wulf, S., Isaia, R., Sottili, G., Cavuoto, G., Galli, P., Messina, P., Sposato, A., Sulpizio, R., and Zanchetta, G.: The late MIS 5 Mediterranean tephra markers: a reappraisal from peninsular Italy terrestrial records, Quaternary Sci. Rev., 56, 31–45, 2012.

Giaccio, B., Arienzo, I., Sottili, G., Castorina, F., Gaeta, M., Nomade, S., Galli, P., and Messina, P.: Isotopic (Sr–Nd) and major element fingerprinting of distal tephras: an application to the Middle-Late Pleistocene markers from the Colli Albani volcano, Central Italy, Quaternary Sci. Rev., 67, 190–206, 2013a.

BGD
12, 15411–15460, 2015

First tephrostratigraphic results of the DEEP site record

N. Leicher et al.

Giaccio, B., Castorina, F., Nomade, S., Scardia, G., Voltaggio, M., and Sagnotti, L.: Revised Chronology of the Sulmona Lacustrine Succession, Central Italy, J. Quaternary Sci., 28, 545–551, 2013b.

Giaccio, B., Galli, P., Peronace, E., Arienzo I., Nomade, S., Cavinato, G. P., Mancini, M., Messina, P., and Sottili, G.: A 560–440 ka tephra record from the Mercure Basin, Southern Italy: volcanological and tephrostratigraphic implications, J. Quaternary Sci., 29, 232–248, 2014.

Giordano, G., De Benedetti, A. A., Diana, A., Diano, G., Gaudioso, F., Marasco, F., Miceli, M., Mollo, S., Cas, R. A. F., and Funiciello, R.: The Colli Albani mafic caldera (Roma, Italy): stratigraphy, structure and petrology, J. Volcanol. Geoth. Res., 155, 49–80, 2006.

Giraudi, C. and Giaccio, B.: The Middle Pleistocene glaciations on the Apennnines (Italy): new chronologcial data and considerations about the preservation of the glacial deposits, Geological Society, London, Special Publications, in press, 2015.

Giraudi, C., Bodrato, G., Lucchi, M. R., Cipriani, N., Villa, I. M., Giaccio, B., and Zuppi, G. M.: Middle and late Pleistocene glaciations in the Campo Felice Basin (central Apennines, Italy), Quaternary Res., 75, 219–230, 2011.

Grant, K. M., Rohling, E. J., Bar-Matthews, M., Ayalon, A., Medina-Elizalde, M., Ramsey, C. B., Satow, C., and Roberts, A. P.: Rapid coupling between ice volume and polar temperature over the past 150,000 years, Nature, 491, 744–747, 2012.

Hamann, Y., Wulf, S., Ersoy, O., Ehrmann, W., Aydar, E., and Schmiedl, G.: First evidence of a distal early Holocene ash layer in Eastern Mediterranean deep-sea sediments derived from the Anatolian volcanic province, Quaternary Res., 73, 497–506, 2010.

Hoffmann, N., Reicherter, K., Fernández-Steeger, T., and Grützner, C.: Evolution of ancient Lake Ohrid: a tectonic perspective, Biogeosciences, 7, 3377–3386, doi:10.5194/bg-7-3377-2010, 2010.

Incarbona, A., Bonomo, S., Di Stefano, E., Zgozi, S., Essarbout, N., Talha, M., Tranchida, G., Bonanno, A., Patti, B., Placenti, F., Buscaino, G., Cuttitta, A., Basilone, G., Bahri, T., Massa, F., Censi, P., and Mazzola, S.: Calcareous nannofossil surface sediment assemblages from the Sicily Channel (central Mediterranean Sea): Palaeoceanographic implications, Mar. Micropaleontol., 67, 297–309, 2008.

Insinga, D. D., Tamburrino, S., Lirer, F., Vezzoli, L., Barra, M., De Lange, G. J., Tiepolo, M., Vallefuoco, M., Mazzola, S., and Sprovieri, M.: Tephrochronology of the astronomically-tuned

KC01B deep-sea core, Ionian Sea: insights into the explosive activity of the Central Mediterranean area during the last 200 ka, Quaternary Sci. Rev., 85, 63–84, 2014.
Iorio, M., Liddicoat, J., Budillon, F., Incoronato, A., Coe, R. S., Insinga, D. D., Cassata, W. S., Lubritto, C., Angelino, A., and Tamburrino, S.: Combined palaeomagnetic secular variation and petrophysical records to time-constrain geological and hazardous events: An example from the eastern Tyrrhenian Sea over the last 120 ka, Global Planet. Change, 113, 91–109, 2014.
Jahns, S. and van den Bogaard, C.: New palynological and tephrostratigraphical investigations of two salt lagoons on the island of Mljet, south Dalmatia, Croatia, Veg. Hist. Archaeobot., 7, 219–234, 1998.
Karkanas, P., White, D., Lane, C. S., Stringer, C., Davies, W., Cullen, V. L., Smith, V. C., Ntinou, M., Tsartsidou, G., and Kyparissi-Apostolika, N.: Tephra correlations and climatic events between the MIS6/5 transition and the beginning of MIS3 in Theopetra Cave, Central Greece, Quaternary Sci. Rev., 118, 170–181, 2015.
Karner, D. B., Juvigne, E., Brancaccio, L., Cinque, A., Ermolli, E. R., Santangelo, N., Bernasconi, S., and Lirer, L.: A potential early middle Pleistocene tephrostratotype for the Mediterranean Basin: the Vallo Di Diano, Campania, Italy, Global Planet. Change, 21, 1–15, 1999.
Karner, D. B., Marra, F., and Renne, P. R.: The history of the Monti Sabatini and Alban Hills volcanoes: groundwork for assessing volcanic-tectonic hazards for Rome, J. Volcanol. Geoth. Res., 107, 185–219, 2001.
Keller, J., Ryan, W. B. F., Ninkovich, D., and Altherr, R.: Explosive volcanic activity in the Mediterranean over the past 200,000 yr as recorded in deep-sea sediments, Geol. Soc. Am. Bull., 89, 591–604, 1978.
Keller, J., Gertisser, R., Reusser, E., and Dietrich, V.: Pumice deposits of the Santorini Lower Pumice 2 eruption on Anafi island, Greece: indications for a Plinian event of exceptional magnitude, J. Volcanol. Geoth. Res., 278, 120–128, 2014.
Kraml, M.: Laser-^{40}Ar/^{39}Ar-Datierungen an distalen marinen Tephren des jung-quartären mediterranen Vulkanismus (Ionisches Meer, METEOR-Fahrt 25/4), Ph.D., Albert-Ludwigs-Universität Freiburg i. Br., 216 pp., 1997.
Kuiper, K. F., Deino, A., Hilgen, F. J., Krijgsman, W., Renne, P. R., and Wijbrans, J. R.: Synchronizing rock clocks of Earth history, Science, 320, 500–504, 2008.

BGD
12, 15411–15460, 2015

Laskar, J., Robutel, P., Joutel, F., Gastineau, M., Correia, A. C. M., and Levrard, B.: A long-term numerical solution for the insolation quantities of the Earth, Astron. Astrophys., 428, 261–285, 2004.

Laurenzi, M. A. and Villa, I.: $^{40}Ar/^{39}Ar$ chronostratigraphy of Vico ignimbrites, Period. Mineral., 56, 285–293, 1987.

Lindhorst, K., Krastel, S., Reicherter, K., Stipp, M., Wagner, B., and Schwenk, T.: Sedimentary and tectonic evolution of Lake Ohrid (Macedonia/Albania), Basin Res., 27, 84–101, 2015.

Lisiecki, L. E. and Raymo, M. E.: A Pliocene-Pleistocene stack of 57 globally distributed benthic $\delta^{18}O$ records, Paleoceanography, 20, PA1003, doi:10.1029/2004PA001071, 2005.

Lourens, L. J.: Revised tuning of Ocean Drilling Program Site 964 and KC01B (Mediterranean) and implications for the $\delta^{18}O$, tephra, calcareous nannofossil, and geomagnetic reversal chronologies of the past 1.1 Myr, Paleoceanography, 19, PA3010, doi:10.1029/2003PA000997, 2004.

Lustrino, M., Duggen, S., and Rosenberg, C. L.: The Central-Western Mediterranean: anomalous igneous activity in an anomalous collisional tectonic setting, Earth-Sci. Rev., 104, 1–40, 2011.

MacDonald, R.: Nomenclature and petrochemistry of the peralkaline oversaturated extrusive rocks, B. Volcanol., 38, 498–516, 1974.

Mahood, G. A. and Hildreth, W.: Geology of the peralkaline volcano at Pantelleria, Strait of Sicily, B. Volcanol., 48, 143–172, 1986.

Marchini, G., Zanchetta, G., Santacroce, R., Vigliotti, L., Capotondi, L., and Sulpizio, R.: Tephrostratigraphy of marine core AD91–17 (Adriatic Sea) Revised, Alpine and Mediterranean Quaternary, 27, 77–84, 2014.

Marciano, R., Munno, R., Petrosino, P., Santangelo, N., Santo, A., and Villa, I.: Late quaternary tephra layers along the Cilento coastline (Southern Italy), J. Volcanol. Geoth. Res., 177, 227–243, 2008.

Margari, V., Pyle, D. M., Bryant, C., and Gibbard, P. L.: Mediterranean tephra stratigraphy revisited: results from a long terrestrial sequence on Lesvos Island, Greece, J. Volcanol. Geoth. Res., 163, 34–54, 2007.

Marianelli, P. and Sbrana, A.: Risultati di misure di standard di minerali e di vetri naturali in microanalisi a dispersione di energia, Atti della Societa Toscana di Scienze Naturali Memorie Serie A, 105, 57–63, 1998.

Marianelli, P., Sbrana, A., and Proto, M.: Magma chamber of the Campi Flegrei supervolcano at the time of eruption of the Campanian Ignimbrite, Geology, 34, 937–940, 2006.
Marra, F., Karner, D. B., Freda, C., Gaeta, M., and Renne, P.: Large mafic eruptions at Alban Hills Volcanic District (Central Italy): chronostratigraphy, petrography and eruptive behavior, J. Volcanol. Geoth. Res., 179, 217–232, 2009.
Marra, F., Deocampo, D., Jackson, M. D., and Ventura, G.: The Alban Hills and Monti Sabatini volcanic products used in ancient Roman masonry (Italy): an integrated stratigraphic, archaeological, environmental and geochemical approach, Earth-Sci. Rev., 108, 115–136, 2011.
Marra, F., Sottili, G., Gaeta, M., Giaccio, B., Jicha, B., Masotta, M., Palladino, D. M., and Deocampo, D. M.: Major explosive activity in the Monti Sabatini Volcanic District (central Italy) over the 800–390 ka interval: geochronological-geochemical overview and tephrostratigraphic implications, Quaternary Sci. Rev., 94, 74–101, 2014.
Matter, M., Anselmetti, F. S., Jordanoska, B., Wagner, B., Wessels, M., and Wüest, A.: Carbonate sedimentation and effects of eutrophication observed at the Kališta subaquatic springs in Lake Ohrid (Macedonia), Biogeosciences, 7, 3755–3767, doi:10.5194/bg-7-3755-2010, 2010.
Matzinger, A., Jordanoski, M., Veljanoska-Sarafiloska, E., Sturm, M., Muller, B., and Wuest, A.: Is Lake Prespa jeopardizing the ecosystem of ancient Lake Ohrid?, Hydrobiologia, 553, 89–109, 2006a.
Matzinger, A., Spirkovski, Z., Patceva, S., and Wuest, A.: Sensitivity of ancient Lake Ohrid to local anthropogenic impacts and global warming, J. Great Lakes Res., 32, 158–179, 2006b.
Mele, D., Sulpizio, R., Dellino, P., and La Volpe, L.: Stratigraphy and eruptive dynamics of a pulsating Plinian eruption of Somma-Vesuvius: the Pomici di Mercato (8900 years BP), B. Volcanol., 73, 257–278, 2011.
Munno, R. and Petrosino, P.: New constraints on the occurence of Y-3 Upper Pleistocene tephra marker layer in the Tyrrhenian Sea, Il Quaternario, 17, 11–20, 2004.
Munno, R. and Petrosino, P.: The late Quaternary tephrostratigraphical record of the San Gregorio Magno Basin (Southern Italy), J. Quaternary Sci., 22, 247–266, 2007.
Narcisi, B. and Vezzoli, L.: Quaternary stratigraphy of distal tephra layers in the Mediterranean – an overview, Global Planet. Change, 21, 31–50, 1999.

BGD
12, 15411–15460, 2015

First tephrostratigraphic results of the DEEP site record

N. Leicher et al.

Nomade, S., Renne, P., Vogel, N., Deino, A., Sharp, W., Becker, T., Jaouni, A., and Mundil, R.: Alder Creek sanidine (ACs-2): a Quaternary $^{40}Ar/^{39}Ar$ dating standard tied to the Cobb Mountain geomagnetic event, Chem. Geol., 218, 315–338, 2005.

Orsi, G., DeVita, S., and diVito, M.: The restless, resurgent Campi Flegrei nested caldera (Italy): Constraints on its evolution and configuration, J. Volcanol. Geoth. Res., 74, 179–214, 1996.

Palladino, D. M., Simei, S., Sottili, G., and Trigila, R.: Integrated approach for the reconstruction of stratigraphy and geology of Quaternary volcanic terrains: an application to the Vulsini Volcanoes (Central Italy), Geol. S. Am. S., 464, 63–84, 2010.

Pappalardo, L., Civetta, L., de Vita, S., Di Vito, M., Orsi, G., Carandente, A., and Fisher, R. V.: Timing of magma extraction during the Campanian Ignimbrite eruption (Campi Flegrei Caldera), J. Volcanol. Geoth. Res., 114, 479–497, 2002.

Paterne, M., Guichard, F., Labeyrie, J., Gillot, P. Y., and Duplessy, J. C.: Tyrrhenian Sea Tephrochronology of the Oxygen Isotope Record for the Past 60,000 Years, Mar. Geol., 72, 259–285, 1986.

Paterne, M., Guichard, F., and Labeyrie, J.: Explosive activity of the South Italian volcanoes during the past 80,000 years as determined by marine tephrochronology, J. Volcanol. Geoth. Res., 34, 153–172, 1988.

Paterne, M., Guichard, F., Duplessy, J. C., Siani, G., Sulpizio, R., and Labeyrie, J.: A 90,000–200,000 yrs marine tephra record of Italian volcanic activity in the Central Mediterranean Sea, J. Volcanol. Geoth. Res., 177, 187–196, 2008.

Peccerillo, A.: Plio-Quaternary Volcanism in Italy: Petrology, Geochemistry, Geodynamics, Springer-Verlag Berlin Heidelberg, 2005.

Petrosino, P., Ermolli, E. R., Donato, P., Jicha, B., Robustelli, G., and Sardella, R.: Using tephrochronology and palynology to date the MIS 13 lacustrine sediments of the Mercure Basin (Southern Apennines – Italy), Italian Journal of Geosciences, 133, 169–186, 2014a.

Petrosino, P., Jicha, B. R., Mazzeo, F. C., and Russo Ermolli, E.: A high resolution tephrochronological record of MIS 14–12 in the Southern Apennines (Acerno Basin, Italy), J. Volcanol. Geoth. Res., 274, 34–50, 2014b.

Petrosino, P., Jicha, B. R., Mazzeo, F. C., Ciaranfi, N., Girone, A., Maiorano, P., and Marino, M.: The Montalbano Jonico marine succession: an archive for distal tephra layers at the Early–Middle Pleistocene boundary in southern Italy, Quatern. Int., in press, 2015.

BGD
12, 15411–15460, 2015

First tephrostratigraphic results of the DEEP site record

N. Leicher et al.

Phillips, D. and Matchan, E.: Ultra-high precision $^{40}Ar/^{39}Ar$ ages for Fish Canyon Tuff and Alder Creek Rhyolite sanidine: new dating standards required?, Geochim. Cosmochim. Ac., 121, 229–239, 2013.
Pross, J., Tzedakis, P. C., Schmiedl, G., Christanis, K., Hooghiemstra, H., Müller, C., Ulrich, K., Ulrich, K., and Stavros, M.: Tenaghi Philippon (Greece) revisited: drilling a continuous lower-latitude terrestirial climate archive of the last 250,000 Years, Scientific Drilling, 5, 44–46, 2007.
Pyle, D. M., Ricketts, G. D., Margari, V., van Andela, T. H., Sinitsyn, A. A., Praslov, N. D., and Lisitsyn, S.: Wide dispersal and deposition of distal tephra during the Pleistocene "Campanian Ignimbrite/Y5" eruption, Italy, Quaternary Sci. Rev., 25, 2713–2728, 2006.
Regattieri, E., Giaccio, B., Zanchetta, G., Drysdale, R. N., Galli, P., Nomade, S., Peronace, E., and Wulf, S.: Hydrological variability over the Apennines during the early last glacial precession minimum, as revealed by a stable isotope record from Sulmona Basin, Central Italy, J. Quaternary Sci., 30, 19–31, 2015.
Reicherter, K., Hoffmann, N., Lindhorst, K., Krastel, S., Fernández-Steeger, T., Grützner, C., and Wiatr, T.: Active basins and neotectonics: morphotectonics of the Lake Ohrid Basin (FYROM and Albania), Z. Dtsch. Ges. Geowiss., 162, 217–234, 2011.
Renne, P. R., Mundil, R., Balco, G., Min, K., and Ludwig, K. R.: Joint determination of ^{40}K decay constants and $^{40}Ar^*/^{40}K$ for the Fish Canyon sanidine standard, and improved accuracy for $^{40}Ar/^{39}Ar$ geochronology, Geochim. Cosmochim. Ac., 74, 5349–5367, 2010.
Robertson, A. and Shallo, M.: Mesozoic–Tertiary tectonic evolution of Albania in its regional Eastern Mediterranean context, Tectonophysics, 316, 197–254, 2000.
Rolandi, G., Bellucci, F., Heizler, M. T., Belkin, H. E., and De Vivo, B.: Tectonic controls on the genesis of ignimbrites from the Campanian Volcanic Zone, Southern Italy, Miner. Petrol., 79, 3–31, 2003.
Rotolo, S. G., Scaillet, S., La Felice, S., and Vita-Sceillet, G.: A revision of the structure and stratigraphgy of pre-Green Tuff ignimbrites at Pantelleria (Strait of Silicy), J. Volcanol. Geoth. Res., 250, 61–74, 2013.
Rouchon, V., Gillot, P. Y., Quidelleur, X., Chiesa, S., and Floris, B.: Temporal evolution of the Roccamonfina volcanic complex (Pleistocene), Central Italy, J. Volcanol. Geoth. Res., 177, 500–514, 2008.
Roulleau, E., Pinti, D. L., Rouchon, V., Quidelleur, X., and Gillot, P.-Y.: Tephro-chronostratigraphy of the lacustrine interglacial record of Piànico, Italian Southern Alps: iden-

BGD
12, 15411–15460, 2015

First tephrostratigraphic results of the DEEP site record

N. Leicher et al.

tifying the volcanic sources using radiogenic isotopes and trace elements, Quatern. Int., 204, 31–43, 2009.
Russo Ermolli, E., Aucelli, P. P. C., Di Rollo, A., Mattei, M., Petrosino, P., Porreca, M., and Rosskopf, C. M.: An integrated stratigraphical approach to the Middle Pleistocene succession of the Sessano Basin (Molise, Italy), Quatern. Int., 225, 114–127, 2010.
Sagnotti, L., Scardia, G., Giaccio, B., Liddicoat, J. C., Nomade, S., Renne, P. R., and Sprain, C. J.: Extremely rapid directional change during Matuyama-Brunhes geomagnetic polarity reversal, Geophys. J. Int., 199, 1110–1124, 2014.
Santacroce, R., Cioni, R., Marianelli, P., Sbrana, A., Sulpizio, R., Zanchetta, G., Donahue, D. J., and Joron, J. L.: Age and whole rock–glass compositions of proximal pyroclastics from the major explosive eruptions of Somma-Vesuvius: a review as a tool for distal tephrostratigraphy, J. Volcanol. Geoth. Res., 177, 1–18, 2008.
Sarna-Wojcicki, A.: Tephrochronology, in: Quaternary Geochronology, edited by: Noller, J. S., Sowers, J. M., and Lettis, W. R., AGU Reference Shelf, American Geophysical Union, Washington, DC, 2013.
Satow, C., Tomlinson, E. L., Grant, K. M., Albert, P. G., Smith, V. C., Manning, C. J., Ottolini, L., Wulf, S., Rohling, E. J., Lowe, J. J., Blockley, S. P. E., and Menzies, M. A.: A new contribution to the late quaternary tephrostratigraphy of the Mediterranean: Aegean Sea core LC21, Quaternary Sci. Rev., 117, 96–112, 2015.
Scaillet, S., Vita-Sceillet, G., and Rotolo, S. G.: Millennial-scale phase relationshhips between ice-core and Mediterranean marine records: insights from high-precision $^{40}Ar/^{39}Ar$ dating of the Green Tuff of Pantelleria, Silicy Strait, Quaternary Sci. Rev., 78, 141–154, 2013.
Sottili, G., Palladino, D. M., and Zanon, V.: Plinian activity during the early eruptive history of the Sabatini volcanic district, Central Italy, J. Volcanol. Geoth. Res., 135, 361–379, 2004.
St. Seymour, K., Christanis, K., Bouzinos, A., Papazisimou, S., Papatheodorou, G., Moran, E., and Denes, G.: Tephrostratigraphy and tephrochronology in the Philippi Peat Basin, Macedonia, Northern Hellas (Greece), Quatern. Int., 121, 53–65, 2004.
Steiger, R. H. and Jäger, E.: Subcommission on geochronology: Convention on the use of decay constants in geo- and cosmochronology, Earth Planet. Sc. Lett., 36, 359–362, 1977.
Stoppa, F., Rosatelli, G., Wall, F., and Jeffries, T.: Geochemistry of carbonatite-silicate pairs in nature: a case history from Central Italy, Lithos, 85, 26–47, 2005.

BGD
12, 15411–15460, 2015

First tephrostratigraphic results of the DEEP site record

N. Leicher et al.

Sulpizio, R., Zanchetta, G., Paterne, M., and Siani, G.: A review of tephrostratigraphy in Central and Southern Italy during the last 65 ka, Il Quaternario – Ital. J. Quaternary Sci., 16, 91–108, 2003.

Sulpizio, R., Bonasia, R., Dellino, P., Di Vito, M. A., La Volpe, L., Mele, D., Zanchetta, G., and Sadori, L.: Discriminating the long distance dispersal of fine ash from sustained columns or near ground ash clouds: the example of the Pomici di Avellino eruption (Somma-Vesuvius, Italy), J. Volcanol. Geoth. Res., 177, 263–276, 2008.

Sulpizio, R., Zanchetta, G., D'Orazio, M., Vogel, H., and Wagner, B.: Tephrostratigraphy and tephrochronology of lakes Ohrid and Prespa, Balkans, Biogeosciences, 7, 3273–3288, doi:10.5194/bg-7-3273-2010, 2010.

Sulpizio, R., Alcicek, M. C., Zanchetta, G., and Solari, L.: Recognition of the Minoan tephra in the Acigöl Basin, Western Turkey: implications for inter-archive correlations and fine ash dispersal, J. Quaternary Sci., 28, 329–335, 2013.

Sumita, M. and Schmincke, H.-U.: Impact of volcanism on the evolution of Lake Van II: temporal evolution of explosive volcanism of Nemrut Volcano (eastern Anatolia) during the past ca. 0.4 Ma, J. Volcanol. Geoth. Res., 253, 15–34, 2013.

Tamburrino, S., Insinga, D. D., Sprovieri, M., Petrosino, P., and Tiepolo, M.: Major and trace element characterization of tephra layers offshore Pantelleria Island: insights into the last 200 ka of volcanic activity and contribution to the Mediterranean tephrochronology, J. Quaternary Sci., 27, 129–140, 2012.

Thunell, R., Federman, A., Sparks, S., and Williams, D.: Age, origin and volcanological significance of the Y-5 ash layer in the Mediterranean, Quaternary Res., 12, 241–253, 1979.

Tomlinson, E. L., Arienzo, I., Civetta, L., Wulf, S., Smith, V. C., Hardiman, M., Lane, C. S., Carandente, A., Orsi, G., Rosi, M., Müller, W., and Menzies, M. A.: Geochemistry of the Phlegraean Fields (Italy) proximal sources for major Mediterranean tephras: implications for the dispersal of Plinian and co-ignimbritic components of explosive eruptions, Geochim. Cosmochim. Ac., 93, 102–128, 2012.

Tomlinson, E. L., Smith, V. C., Albert, P. G., Aydar, E., Civetta, L., Cioni, R., Çubukçu, E., Gertisser, R., Isaia, R., Menzies, M. A., Orsi, G., Rosi, M., and Zanchetta, G.: The major and trace element glass compositions of the productive Mediterranean volcanic sources: tools for correlating distal tephra layers in and around Europe, Quaternary Sci. Rev., 118, 48–66, 2015.

BGD
12, 15411–15460, 2015

First tephrostratigraphic results of the DEEP site record

N. Leicher et al.

Ton-That, T., Singer, B., and Paterne, M.: $^{40}Ar/^{39}Ar$ dating of latest Pleistocene (41 ka) marine tephra in the Mediterranean Sea: implications for global climate records, Earth Planet. Sc. Lett., 184, 645–658, 2001.
Turbeville, B. N.: Tephra fountaining, rheomorphism, and spatter flow during emplacement of the Pitigliano Tuffs, Latera-Caldera, Italy, J. Volcanol. Geoth. Res., 53, 309–327, 1992a.
Turbeville, B. N.: $^{40}Ar/^{39}Ar$ Ages and stratigraphy of the Latera caldera, Italy, B. Volcanol., 55, 110–118, 1992b.
Tzedakis, P. C.: Long-term tree populations in northwest Greece through multiple quaternary climatic cycles, Nature, 364, 437–440, 1993.
Vezzoli, L.: Tephra layers in Bannock Basin (Eastern Mediterranean), Mar. Geol., 100, 21–34, 1991.
Vogel, H., Zanchetta, G., Sulpizio, R., Wagner, B., and Nowaczyk, N.: A tephrostratigraphic record for the last glacial-interglacial cycle from Lake Ohrid, Albania and Macedonia, J. Quaternary Sci., 25, 320–338, 2010.
Wagner, B., Reicherter, K., Daut, G., Wessels, M., Matzinger, A., Schwalb, A., Spirkovski, Z., and Sanxhaku, M.: The potential of Lake Ohrid for long-term palaeoenvironmental reconstructions, Palaeogeogr. Palaeocl., 259, 341–356, 2008.
Wagner, B., Vogel, H., Zanchetta, G., and Sulpizio, R.: Environmental change within the Balkan region during the past ca. 50 ka recorded in the sediments from lakes Prespa and Ohrid, Biogeosciences, 7, 3187–3198, doi:10.5194/bg-7-3187-2010, 2010.
Wagner, B., Francke, A., Sulpizio, R., Zanchetta, G., Lindhorst, K., Krastel, S., Vogel, H., Rethemeyer, J., Daut, G., Grazhdani, A., Lushaj, B., and Trajanovski, S.: Possible earthquake trigger for 6th century mass wasting deposit at Lake Ohrid (Macedonia/Albania), Clim. Past, 8, 2069–2078, doi:10.5194/cp-8-2069-2012, 2012.
Wagner, B., Wilke, T., Krastel, S., Zanchetta, G., Sulpizio, R., Reicherter, K., Leng, M. J., Grazhdani, A., Trajanovski, S., Francke, A., Lindhorst, K., Levkov, Z., Cvetkoska, A., Reed, J. M., Zhang, X., Lacey, J. H., Wonik, T., Baumgarten, H., and Vogel, H.: The SCOPSCO drilling project recovers more than 1.2 million years of history from Lake Ohrid, Scientific Drilling, 17, 19–29, 2014.
Washington, H. S.: The Roman comagmatic region, Carnegie Institution of Washington, 1906.
Watzin, M. C., Puka, V., and Naumoski, T. B.: Lake Ohrid and Its Watershed: Our Lake, Our Future. A State of the Environment Report., Hydrobiological Institute, Tirana, Albania and Ohrid, Macedonia, 134 pp., 2002.

Wulf, S., Kraml, M., Brauer, A., Keller, J., and Negendank, J. F. W.: Tephrochronology of the 100 ka lacustrine sediment record of Lago Grande di Monticchio (Southern Italy), Quatern. Int., 122, 7–30, 2004.
Wulf, S., Brauer, A., Mingram, J., Zolitschka, B., and Negendank, J. F. W.: Distal tephras in the sediments of Monticchio maar lakes, In: Geologia del Monte Vulture, Bollettino della Societa Geologica Italiana, ed. by: Principe, C., 105–122 2006.
Wulf, S., Keller, J., Paterne, M., Mingram, J., Lauterbach, S., Opitz, S., Sottili, G., Giaccio, B., Albert, P. G., Satow, C., Tomlinson, E. L., Viccaro, M., and Brauer, A.: The 100–133 ka record of Italian explosive volcanism and revised tephrochronology of Lago Grande di Monticchio, Quaternary Sci. Rev., 58, 104–123, 2012.
Zanchetta, G., Sulpizio, R., Giaccio, B., Siani, G., Paterne, M., Wulf, S., and D'Orazio, M.: The Y-3 tephra: A last glacial stratigraphic marker for the Central Mediterranean Basin, J. Volcanol. Geoth. Res., 177, 145–154, 2008.
Zanchetta, G., Sulpizio, R., Roberts, N., Cioni, R., Eastwood, W. J., Siani, G., Caron, B., Paterne, M., and Santacroce, R.: Tephrostratigraphy, chronology and climatic events of the Mediterranean basin during the Holocene: an overview, Holocene, 21, 33–52, 2011.
Zanchetta, G., Regattieri, E., Giaccio, B., Wagner, B., Sulpizio, R., Vogel, H., Sadori, L., Masi, A., Sinopoli, G., Leng, M. J., Lacey, J. H., Francke, A., and Leicher, N.: Aligning MIS5 proxy records from Lake Ohrid (FYORM) with Mediterranean independently-dated archives: implication for core chronology, Biogeosciences, in press, 2015.

BGD
12, 15411–15460, 2015

Table 1. Average major element glass composition (normalised to 100 %) of investigated tephras OH-DP-0115–OH-DP-2060 of the DEEP site sequence. All data were obtained using WDS, except for OH-DP-1817*, which is based on EDS measurements. The full dataset is given in the Supplement.

Tephra		SiO_2	TiO_2	Al_2O_3	FeO_{TOT}	MnO	MgO	CaO	Na_2O	K_2O	P_2O_5	F	Cl	SO_3	Total	Tot. Alkali	Alk. Ratio
OH-DP-0115	$\bar{x}$	61.35	0.42	18.27	3.60	0.13	0.78	2.84	3.34	9.16	0.12	0.14	0.46	0.10	95.25	12.49	2.77
n = 17	*s*	1.32	0.15	0.21	0.74	0.05	0.35	0.76	0.57	0.79	0.09	0.09	0.10	0.06	2.16	1.06	0.45
OH-DP-0169b	$\bar{x}$	61.76	0.43	18.86	3.01	0.25	0.36	1.86	5.96	7.47	0.04	0.33	0.83	0.05	97.04	13.43	1.26
n = 18	*s*	0.31	30.67	9.22	7.93	1.38	0.06	0.75	2.05	0.81	3.72	0.15	0.26	0.39	1.25	0.31	0.07
OH-DP-0169a	$\bar{x}$	61.69	0.41	18.89	3.04	0.26	0.34	1.78	6.28	7.28	0.04	0.36	0.85	0.05	98.78	13.56	1.17
n = 25	*s*	0.44	0.03	0.14	0.09	0.04	0.02	0.04	0.56	0.15	0.02	0.07	0.04	0.02	1.56	0.57	0.17
OH-DP-0404	$\bar{x}$	57.49	0.54	19.05	5.10	0.17	1.30	4.33	4.06	7.72	0.24	0.18	0.50	0.09	97.08	11.78	1.93
n = 20	*s*	1.00	0.11	0.45	0.67	0.04	0.24	0.65	0.54	0.62	0.07	0.08	0.09	0.05	1.33	0.93	0.25
OH-DP-0435	$\bar{x}$	61.06	0.45	18.53	3.09	0.30	0.36	1.78	6.12	6.98	0.05	0.37	0.86	0.05	96.82	13.10	1.16
n = 22	*s*	0.34	0.04	0.17	0.12	0.10	0.09	0.10	0.52	0.55	0.03	0.13	0.14	0.03	1.60	0.26	0.20
OH-DP-0499 (trachyte)	$\bar{x}$	65.32	0.69	15.32	6.02	0.28	0.33	1.32	5.68	4.92	0.11	0.08	0.15	0.06	97.13	10.61	0.87
n = 11	*s*	1.06	0.08	0.88	0.31	0.04	0.09	0.25	0.36	0.09	0.04	0.05	0.05	0.02	1.70	0.41	0.05
OH-DP-0499 (pantellerite)	$\bar{x}$	73.61	0.36	8.77	7.30	0.34	0.08	0.33	4.72	4.46	0.02	0.29	0.85	0.06	93.33	9.18	0.95
n = 32	*s*	0.34	0.03	0.21	0.15	0.05	0.02	0.03	0.28	0.09	0.02	0.09	0.07	0.03	1.16	0.28	0.06
OH-DP-0617	$\bar{x}$	60.15	0.43	19.77	2.75	0.15	0.42	2.38	5.04	8.85	0.05	0.49	0.24	0.12	94.36	13.89	1.76
n = 13	*s*	0.33	0.02	0.28	0.09	0.04	0.02	0.06	0.16	0.26	0.02	0.10	0.02	0.04	1.62	0.16	0.10
OH-DP-0624	$\bar{x}$	51.40	1.02	18.17	8.00	0.19	3.09	8.36	3.20	5.88	0.68	0.19	0.34	0.37	97.77	9.08	1.84
n = 19	*s*	3.60	0.22	0.62	2.13	0.03	1.17	2.48	0.68	1.45	0.28	0.06	0.08	0.17	1.29	2.08	0.18
OH-DP-1817*	$\bar{x}$	43.36	1.26	15.53	11.28	0.30	5.23	13.72	3.51	5.24	0.45	–	0.12	–	100.00	8.75	1.55
n = 10	*s*	1.05	0.14	0.69	0.60	0.10	0.25	0.94	0.66	0.56	0.17	–	0.05	–	–	0.85	0.31
OH-DP-1955	$\bar{x}$	57.53	0.57	20.51	4.03	0.18	0.56	4.55	4.78	6.97	0.09	0.31	0.23	0.21	96.70	11.75	1.47
n = 18	*s*	1.49	0.10	0.47	0.34	0.04	0.07	0.52	0.72	1.55	0.02	0.11	0.05	0.05	1.83	1.90	0.33
OH-DP-2010	$\bar{x}$	54.03	0.76	18.14	6.33	0.15	1.77	6.23	3.08	8.66	0.35	0.32	0.08	0.49	97.59	11.73	2.87
n = 22	*s*	3.62	0.17	0.72	1.75	0.03	0.81	1.81	0.49	0.89	0.19	0.11	0.03	0.16	1.77	1.10	0.43
OH-DP-2017	$\bar{x}$	64.43	0.44	18.27	2.59	0.18	0.29	1.06	5.65	6.32	0.05	0.24	0.36	0.11	94.22	11.97	0.29
n = 21	*s*	0.20	0.08	0.12	0.08	0.03	0.02	0.05	0.26	0.14	0.03	0.07	0.02	0.03	0.60	1.12	0.06
OH-DP-2060	$\bar{x}$	44.94	0.78	18.67	8.44	0.29	1.61	10.91	5.39	7.74	0.28	0.91	0.19	0.95	96.34	13.13	1.46
n = 19	*s*	1.70	0.17	0.94	1.18	0.05	0.98	1.26	0.76	1.32	0.16	0.23	0.04	0.48	1.81	1.68	0.27

BGD

12, 15411–15460, 2015

First tephrostratigraphic results of the DEEP site record

N. Leicher et al.

Table 2. Depths and ages of tephras in the DEEP site succession. $^{40}Ar/^{39}Ar$ ages (last column) are recalculated relative to ACs-2 at 1.193 Ma (Nomade et al., 2005) and the total decay constant of Steiger and Jäger (1977), with uncertainties given at 2σ. Tephra layers in bold are not considered for the age-depth modelling (Francke et al., 2015).

Tephra DEEP site	Depth (mcd)	Eruption/Tephra	Age (ka)	References	recalculated $^{40}Ar/^{39}Ar$ ages
OH-DP-0027	2.773	Mercato	8.43–8.63	Zanchetta et al., 2011	N.A.
OH-DP-0115	11.507	Y-3	28.68–29.42	Albert et al., 2015	N.A.
OH-DP-0169	16.933	Campanian Ignimbrite/Y-5	39.28± 0.1	De Vivo et al., 2001	39.6 ± 0.1
OH-DP-0404	**40.486**	**POP2**	**102 ± 2.4**	**Regattieri et al., 2015**	**N.A.**
OH-DP-0435	43.513	X-6	109 ± 2	Iori et al., 2014	109 ± 2
OH-DP-0499	49.947	P-11	129 ± 6	Rotolo et al., 2013	129 ± 6
OH-DP-0617	61.726	Vico "Ignimbrite B"	157 ± 3	Laurenzi and Villa, 1987	162 ± 6
OH-DP-0624	**62.413**	**Pitigliano Tuff**	**158 ± 22**	**Turbeville, 1992a**	**163 ± 22**
OH-DP-1817	181.769	Pozzolane Rosse	457 ± 8	Karner et al., 2001	457 ± 8
			457 ± 2	Giaccio et al., 2013	457 ± 2
OH-DP-1955	**195.566**	**SC5**	**493.1 ± 10.9**	**Giaccio et al., 2014**	–
OH-DP-2010	**201.049**	**Sabatini Fall A**	**499 ± 3**	**Marra et al., 2014**	**496 ± 3**
OH-DP-2017	201.782	Acerno A11-12	514 ± 6	Petrosino et al., 2014	511 ± 6
OH-DP-2060	**206.080**	**Tufo di Bagni Albule**	**527 ± 2**	**Marra et al., 2009**	–

BGD
12, 15411–15460, 2015

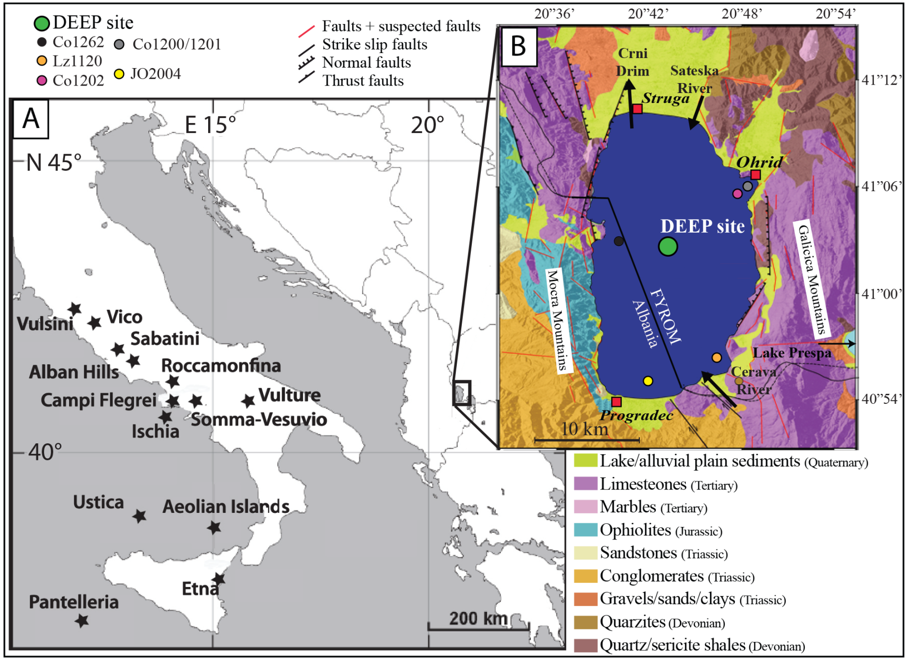

Figure 1. (a) Location of Lake Ohrid in the Mediterranean region and of the Italian volcanoes. **(b)** Geological map of the Lake Ohrid catchment modified after Lindhorst et al. (2015) and the core location from previous studies (Lz1120, Co1200/1201/1202/1262, and JO2004) and the ICDP main drill site DEEP.

BGD
12, 15411–15460, 2015

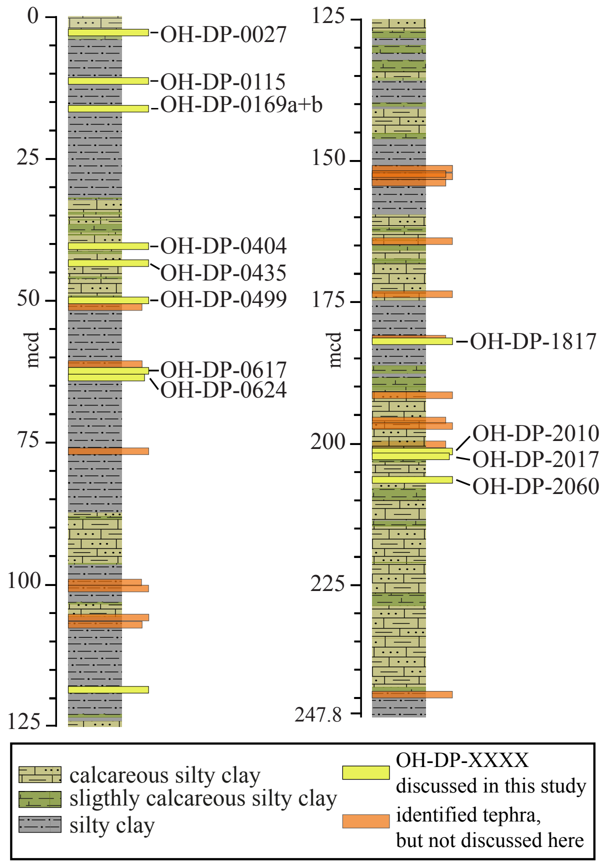

Figure 2. (Litho-) Stratigraphy of the uppermost 247.8 mcd of the DEEP site sequence and the position of identified tephras. Thickness of tephra layers is not to scale, more detailed information about tephra thickness are provided in the text.

BGD
12, 15411–15460, 2015

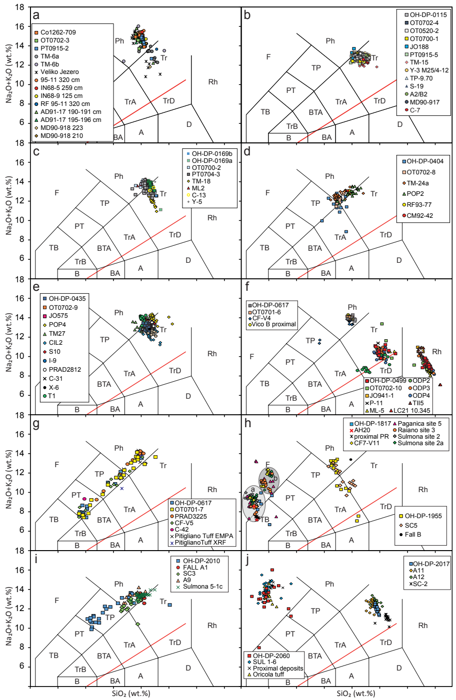

Figure 3. Total alkali-silica diagram (Bas et al., 1986) to classify and correlate the DEEP site tephra layers OH-DP-0027–OH-DP-2060 **(a–j)**. The full dataset of the DEEP site record is given in Table 1 and in the supplementary online material. For references of correlated tephras, see text.

BGD
12, 15411–15460, 2015

First tephrostratigraphic results of the DEEP site record

N. Leicher et al.

Title Page
Abstract | Introduction
Conclusions | References
Tables | Figures
◀◀ | ▶▶
◀ | ▶
Back | Close
Full Screen / Esc
Printer-friendly Version
Interactive Discussion

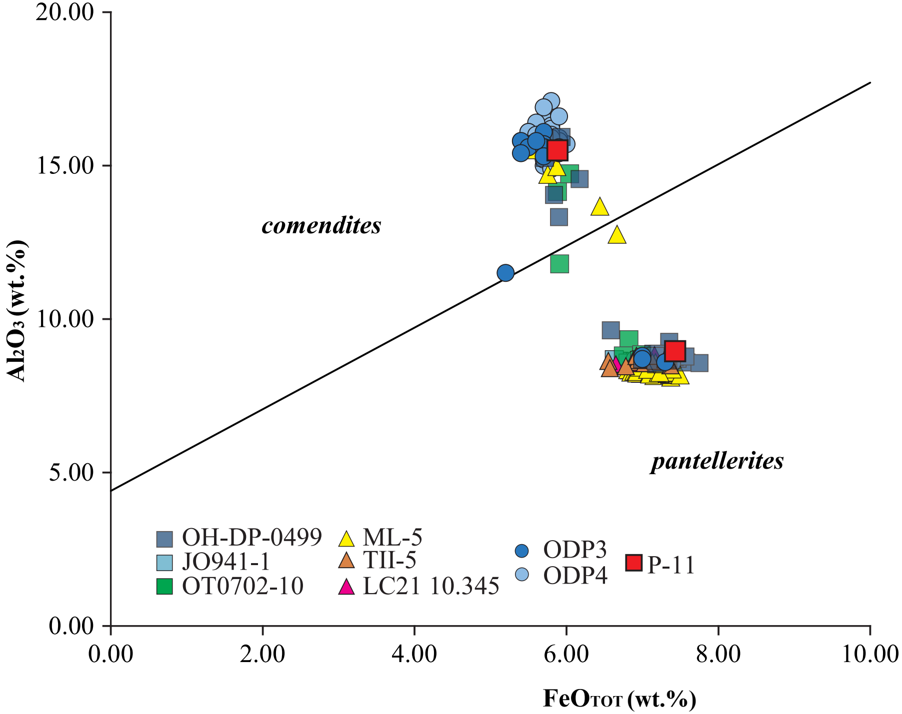

Figure 4. Al_2O_3-FeO_{TOT} diagram for classification of comendites and pantellerites according to MacDonald (1974). Tephra OH-DP-0499 and most of the other P-11 equivalents show the typical bimodal chemical composition of P-11, except for the very distal equivalents LC21 10.345 and THP-TII5, which only have a pantelleritic part (see text for data references).

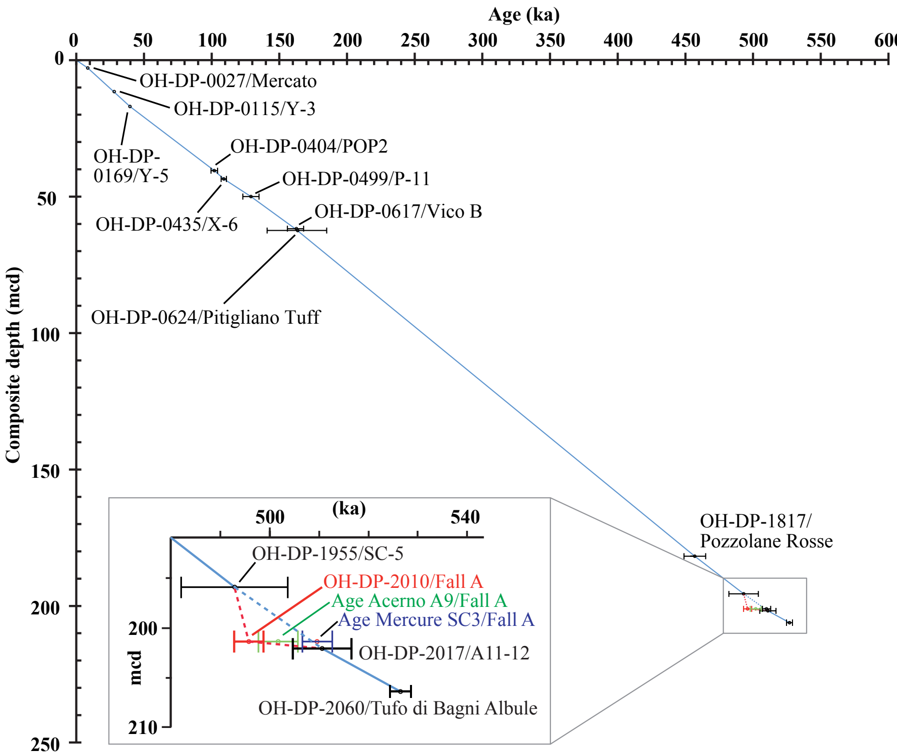

Figure 5. Age-depth plot for the selected DEEP site tephras. The ages of the tephras are based on recalculation of existing $^{40}Ar/^{39}Ar$ ages (Table 2) or according to published data for non $^{40}Ar/^{39}Ar$ ages. Chronological tie points were interpolated on a linear basis (blue line). The dotted lines in the insert indicate a suspicious change in the sedimentation rate for a different age of the Fall A tephra.